https://doi.org/10.1016/j.jcis.2016.08.009

The effects of intermolecular interactions on the physical properties of organogels in edible oils

Francesca R. Lupi[1], *Valeria Greco*[1], *Noemi Baldino*[1], *Bruno de Cindio*[1], *Peter Fischer*[2], *Domenico Gabriele*[1]

[1] Department of Information, Modeling, Electronics and System Engineering, (D.I.M.E.S.) University of Calabria, Via P. Bucci, Cubo 39C, I-87036 Rende (CS), Italy

francesca.lupi@unical.it; valeria.greco@unical.it; noemi.baldino@unical.it, bruno.decindio@unical.it, domenico.gabriele@unical.it

[2] Institute of Food, Nutrition and Health, ETH Zurich, 8092 Zurich, Switzerland

peter.fischer@hest.ethz.ch

Corresponding author

Dr. Domenico Gabriele

Department of Information, Modeling, Electronics and System Engineering (D.I.M.E.S.)

Via P. Bucci – Cubo 39C

I-87036 Arcavacata di Rende (CS), Italy

Email: domenico.gabriele@unical.it

Tel. +39 0984 496687; Fax +39 0984 494009

ABSTRACT

The microstructure of organogels based on monoglycerides of fatty acids (MAGs) and policosanol and on different edible oils was investigated by using different techniques (calorimetry, nuclear magnetic resonance, infrared spectroscopy, rheology, polarized light microscopy) towards a better understanding and control of the oil gelation phenomena. Dynamic moduli were related via a fractal model to microstructural information such as solid content and fractal dimension. Infrared spectroscopy evidenced that network structure in MAGs gel is mainly due to hydrogen bonding, whereas in policosanol system is mainly given by van der Waals interactions. Because of the different relative contribution of molecular interactions, the investigated organogelators exhibit a distinguished macroscopic behavior. MAGs are sensitive to the utilized oil and structuration occurs quickly, even though at a temperature lower than policosanol. Policosanol organogels exhibit a behavior independent of the used oil and a slower gelation rate, as a result of the weaker van der Waals interactions. Nevertheless, at lower concentration a stronger final gel is obtained, probably due to of the large number of interactions arising among the long alkyl chains of the fatty alcohols. Obtained results evidenced that policosanol is very effective in gelation of different oils and seems promising for potential commercial uses.

Keywords: *organogel; edible oils; monoglycerides of fatty acids; policosanol; FT-IR; DSC; van der Waals interactions; hydrogen bonding; rheology*

1. INTRODUCTION

Organogels or oleogels are innovative materials considered as valuable substitutes for reducing saturated or *trans* fats in food industry [1-3] as well as rheological modifiers in cosmetical or pharmaceutical formulations [4]. In food applications, edible oil organogels are one of the most promising alternatives for designing new hardstocks without the addition of hydrogenated or saturated fats. A wide body of literature reports on the use of different organogels in food materials: Zetzl et al.[5] used ethylcellulose gels for substituting saturated fats in frankfurters, Lupi et al. used monoglycerides of fatty acids (MAGs), fatty alcohols or soy lecithin for structuring meat sauces [6, 7], Toro-Vazquez et al. [8] described the use of MAGs and waxes oleogels for hardening water-in-oil food emulsions. Various other food applications of different organogels were reviewed by Co and Marangoni [3], Wang et al. [9], and Patel & Dewettinck [10]. In cosmetical or pharmaceutical applications organogels are mainly used as carriers for controlled drug delivery in oral [11, 12] or topical [13-15] uses because of their ability to dissolve lipophilic components and to release them with a controlled rate depending on the organogel's rheological properties.

Organogels can be categorized by the carbon chain length of the used organogelators. Organogelators can be divided into LMWO (low molecular weight, up to C_{36} [16]) or PO (polymeric, with longer chains). In food applications, LMWOs are more commonly used than POs, due to their ability to provide structure to vegetable oils and for being edible. Even though these systems are investigated from rheological, chemical, physical, and microstructural point of view, knowledge about the gelation mechanism is still missing. It seems evident that the network structure is based on noncovalent forces such as van der Waals interactions, dipole-dipole interactions [17-20], and predominantly by hydrogen bonding (H-bonding) [18, 21]. According to the different interaction potential, organogelators are usually classified between hydrogen-bond-based and nonhydrogen-bond-based compounds [20].

Monoglycerides of fatty acids (MAGs) are a typical example of edible hydrogen-bond-based gelators [22] and they are among the rare systems capable of self-assembling both in aqueous and organic media [23, 24]. Aqueous solutions of MAG form different liquid crystalline mesophases upon cooling and in ternary MAG/oil/water systems, the presence of water usually dominates the behavior of structuring MAG [25, 26]. On the contrary, the phase behavior of MAG in hydrophobic solvents in less studied. Da Pieve et al. [27] analyzed MAG/cod liver oil gels using a polarizing light microscope and showed a needle-like morphology of MAG crystals. Kesselman and Shimoni [28] confirmed this result for MAG/olive oil gels and reported the formation of additional spherulitic or rosette-like microstructure using corn oil as the solvent. It is suggested that the oil influences the microstructural features of MAG crystals or as reported by Co and Marangoni [3] the differences in MAG crystal morphology may be also attributed to the presence of impurities in the oil. From a rheological point of view, several papers are available on MAGs behavior describing both oscillation [3, 29-31] and shear properties [32].

In recent years, several other organogelators were studied to gel edible oils, mainly based on waxes, fatty alcohols [11, 29, 33, 34], and their mixtures with other gelators [8, 35]. For example, Schaink et al. [36] investigated the gelling capabilities of a mixture of stearic acid and stearic alcohol in sunflower oil. Gandolfo et al. [37] studied the oil-structuring potential of fatty acids, fatty alcohols and their mixture in sunflower, soybean, and rapeseed oil. The authors observed also the synergistic effect given by mixtures of gelators with the same chain lengths. Lupi et al. [29] investigated the potential structuring effect of policosanol, a mixture of fatty alcohols in which the major component is octacosanol in olive oil. The same authors investigated policosanol organogels to produce carriers for ferulic acid delivery by ingestion [11]. This gelator seems particularly promising because it is already used as dietary supplement and is able to gel edible oils in relatively small amounts [29].

The present paper reports on the self-assembly of MAGs and policosanol organogels with different techniques such as rheology, infra-red spectroscopy (FT-IR), DSC (differential scanning

calorimetry), NMR (nuclear magnetic resonance), and polarized light microscopy with a rheo-optical system. Although MAGs are widely used and studied, a systematic and comprehensive investigation of their properties and microstructure is still missing. Policosanol was only recently investigated and detailed information on gelation phenomena and intermolecular interactions is not yet available. The comparison of policosanol to better known gelators such as MAGs, aims towards a more generic understanding of the gelling behavior and the resulting microstructure and rheology of organogels. The effect of different edible oils was investigated to evaluate potential differences in gelation phenomena depending on solvent-gelator interactions.

2. MATERIALS AND METHODS

2.1 Materials and samples preparation

Organogels were produced with commercial virgin olive oil ('V', De Santis, Italy), extra-virgin olive ('E', Gabro, Italy), and sunflower oil ('S', De Santis, Italy). As first organogelator, a commercial MAG ('M') as a mixture of monoglycerides of fatty acids with an equal mass fraction of monopalmitin and monostearin (Myverol 18-04K, Kerry Group, Ireland) was used. As second organogelator, policosanol ('P') from rice bran wax (composed of 60%w/w octacosanol [29], A.C.E.F., Italy) was utilized. Sample notation indicate the oil and organogelator along with the concentration X of the respected organogelator. For example $VM_{0.03}$ would be a virgin olive oil gelled with 0.03 weight fraction of MAG. All samples were prepared in a water bath thermostated by a plate heater (Jolly 2, Falc Instruments, Italy) adding the organogelator to the oil previously heated up to 70°C for MAG-gelled samples and 85°C for VP samples. The system was continuously stirred using a laboratory mixer (RW 20, IKA, Germany) and maintained at the temperature of preparation until tests were performed. Investigated samples are reported in Table 1.

2.2 Rheological measurement

120 *2.2.1 Oscillatory and Shear Rheology.*

121 VM samples were analyzed with a controlled strain rheometer ARES-RFS (TA Instruments,
122 USA) equipped with a parallel plate geometry (diameter = 50 mm, gap = 1 ± 0.1 mm) whereas
123 VP samples were studied with a DSR-200 (Rheometric Scientific, U.S.A.) equipped with a
124 parallel plate geometry (diameter = 40mm, gap = 1 ± 0.1 mm). Organogels are highly
125 temperature-dependent materials and, therefore, the temperature of the lower plate was carefully
126 controlled by a Peltier system (± 0.1°C). Temperature ramp tests (time cure) were performed in
127 linear viscoelastic regime from 70°C to 10°C in the case of VM samples and from 85°C to 20°C
128 for VP samples applying a cooling rate of -1°C/min [29, 30]. Lower final temperatures (down to
129 0°C) were applied to samples exhibiting a low onset of crystallization (lower than 10°C). Two
130 parameters, T_{co} and T_g, were estimated from the analysis of the obtained temperature ramp tests.
131 The onset of crystallization temperature (T_{co}) was calculated following the procedure described
132 by Lupi et al. [30], as the temperature at which a strong increase of the complex modulus G* and,
133 thus, a sudden decrease of loss tangent was observed. The gelation point (T_g) was identified as
134 the crossover of both dynamic moduli, i.e. where the loss tangent is equal to unity [29, 30].
135 Considering that, for samples having a gelator fraction greater than a threshold, these two
136 parameters can be nearly equal, differences among them were analyzed using t-student test
137 (Statgraphics Centurion XV, USA). They were assumed to be significant at p-value 0.01 (interval
138 of confidence of 99%). All data fitting was carried out with Table Curve 2D Software (Jandel
139 Scientific, USA).

140 To rationalize differences in the final microstructure and the gelling kinetics towards such final
141 structure, an average non-isothermal structure development rate (*SDr*) was defined. The average
142 *SDr* in the time interval between times t_1 and t_2 can be estimated as [38]:

143 $$SDr = \frac{1}{t_1 - t_2} \int_{t_1}^{t_2} \left(\frac{dG'}{dt} \right) dt \qquad (1)$$

The starting time t_1 was considered as the time at which the temperature is equal to T_{co}, whereas t_2 corresponds to the time at which the temperature value of T_{25} is reached. Here T_{25} is defined as T_{co} - 25°C. The average *SDr* was calculated as shown in the following equation:

$$SDr = \frac{1}{t(T_{co}) - t(T_{25})} \int_{t(T_{co})}^{t(T_{25})} \left(\frac{dG'}{dt} \right) dt \quad (2)$$

The first derivative of the elastic modulus *G'* with respect to time was calculated for each temperature ramp tests using a forward-difference numerical method and the integral between two consecutive points was evaluated using the trapezoidal rule.

2.2.2 Rheo-optical Experiments

The effects of different vegetable oils on the properties of organogels were investigated with temperature ramp tests carried out with a stress-controlled rheometer (HAAKE MARS III, Thermo Scientific, Germany) equipped with a RheoScope module (camera Foculus FO232 TB monochrome, magnification of the lens 20X, Thermo Scientific, Germany). A parallel plate geometry (diameter = 50 mm, gap = 1 ± 0.1mm) with a polished upper plate was used. Images were recorded at different temperature levels during rheological measurements.

2.3 Thermal analysis

The crystallization and melting thermograms were obtained by using a DSC set up (DSC 822e, Mettler Toledo, Switzerland). Samples (≈ 5 - 10 mg) were sealed in aluminum pans, kept at 70°C or 85°C (for VM and VP samples, respectively) for 20 minutes to erase a potential previous thermal history, and then cooled to 0°C at a rate of 1°C/min, while recording the heat flux as a function of temperature. After 1 minute at 0°C, the material was heated up to 70°C (or 85°C) using the same thermal ramp and recording the heat flux. As reported by Toro-Vazquez et al. [39], the onset of crystallization temperature evaluated by DSC ($T_{co,DSC}$) was estimated as the temperature corresponding to the beginning of the first exothermic peak, while the crystal melting temperature (T_M) was considered as the temperature corresponding to the peak of the melting

endotherm. The heat of crystallization (ΔH_c) and the heat of melting (ΔH_m) were computed as the areas under the crystallization exotherm and melting endotherm, respectively [40].

2.4 Spectroscopic analysis

The solid fat content (SFC) of organogels was determined by low-frequency nuclear magnetic resonance (Minispec mq20, Bruker, Germany) in the temperature range from preparation temperature down to 20°C. Thus, organogels formation was obtained directly in NMR tubes using the same thermal history as for the rheological and thermal characterization. Temperature was controlled with an external water bath (RC 20, LAUDA-Brinkmann LP., USA) that provided an average cooling rate approximately equal to 1°C/min. SFC was measured at different temperature values during gel formation. For samples with low fractions of organogelators results were corrupted by the small amount of solids present at the investigated temperatures and therefore are not shown. In these cases, the onset of crystallization temperature ($T_{co,NMR}$) was defined as the temperature at which a sudden increase of the SFC versus temperature was observed.

Infrared absorption spectra were recorded using a Nicolet iS-10 FT-IR spectrometer (Thermo Scientific, USA) equipped with a Smart iTX ATR sampling accessory. Samples were prepared at 70°C or 85°C according to the procedure previously described and allowed to cool at room temperature (approximately 25°C). Then, spectra were obtained within the range of wavenumber between 400 and 4000 cm^{-1}.

3. RESULTS AND DISCUSSION

3.1 Effects of gelators on properties of olive oil based gels

3.1.1 Rheological characterization of samples

Organogels exhibit a typical behavior during temperature ramp test when decreasing the temperature [29-31] as shown for sample $VM_{0.034}$ in Fig. 1. At high temperatures ($T > T_{co}$), the

system is completely molten and shows a viscous behavior, whereas, at T_{co}, a sudden increase in complex modulus curve is observed, indicating the beginning of crystallization. Cooling the sample, interactions between crystalline aggregates arise and extend over the entire sample, resulting in the formation of a 3-D crystalline gel network. The temperature at which the *G'/G''* crossover is observed has been identified as the gelation point (T_g) [30]. At lower temperature ($T < T_g$), the system behaves as a solid-like gel material with G^* slightly increasing with decreasing temperature. A slope change in the G^* curve can be observed at approximately 15°C suggesting a potential transition to a second crystal polymorph as also observed by Ojijo et al. [31]. This variation in the rheological properties is discussed later, comparing rheological results with those obtained from thermal and spectroscopic analysis.

Aiming at investigating the crystallization and gelation phenomena promoted by the organogelator, a wide range of gelator concentrations was studied. The estimated T_{co} and T_g values for all samples are listed in Table 1. The results show that both the parameters increase with increasing organogelator concentration, with an asymptotic trend of T_{co} at high organogelator concentrations. These results are in agreement with literature data [31] and can be attributed to the high organogelator concentrations that cause a higher degree of supersaturation accelerating the nucleation and the subsequent gelation. In a similar way Lopez-Martinez et al. [41] observed that, when the organogelator concentration is low, a higher supercooling is required to develop a gel [41]. The crossover between the dynamic moduli was always observed for samples VM, even for those produced with the lowest amounts of gelators, indicating that the minimum fraction required for gelation is very small, lower than $X_M = 0.001$. On the other hand for samples VP, the crossover was observed only for fractions larger than $X_P = 0.005$. Lupi et al. [30] analyzed systems produced with Myverol, carrying out time cure tests with a cooling rate of 5° C/min. They observed that crystallization occurred only for organogelator fractions larger than a critical value ranging between $X_M = 0.001$ and 0.005, whereas the critical threshold for gelation was between $X_M = 0.01$ and 0.015. For VM samples, at X_M lower than 0.034, T_{co} was significantly higher than

T_g but with increasing the gelator mass fractions, the system forms a network immediately after the onset of crystallization. The same behavior was observed for samples VP with a threshold mass fraction equal to $X_P = 0.025$.

The average *SDr* provides information on the rate of storage modulus increase during cooling of self-assembling structuring agents. The changes observed in rheological properties during temperature ramp tests are closely related to changes in the system microstructure occurring upon cooling. Fig. 2 reports on the obtained values for both organogels at X = 0.03 (w/w) fraction. The data suggest that fatty alcohols facilitate, during cooling, a faster gelation than monoglycerides and thus the potential presence of different intermolecular interactions.

3.1.2 Thermal analysis

DSC thermograms generally exhibit a similar trend. Fig. 3a displays the results obtained for pure organogelator in comparison with samples $VM_{0.015}$, $VM_{0.034}$ and $VM_{0.300}$ (X_M = 0.015, 0.034, and 0.300). The crystallization curve of pure organogelator (Myverol) showed two exotherms (65.97 ± 0.08°C and 14.05 ± 0.03°C) with approximately the same values as found by López-Martínez et al. [41] for commercial mixtures of MAGs. The enthalpy of crystallization, associated to the first peak, was found equal to 91.0±0.5 J/g. Both peaks correspond to the crystallization into a lamellar structure and the polymorphic transition into sub-α structure. It is known that 1-mono-stearoyl glycerol (glyceryl monostearate) and 1-mono-palmitoyl-glycerol (glyceryl monopalmitate) often co-crystallize in a mixed lamellar structure [41]. A similar behavior has been observed for other commercial mixtures of monoglycerides such as glyceryl monostearate (92% w/w) [26] and other mixtures of C_{16} and C_{18} monoglycerides [41, 42]. Upon further cooling, the aliphatic tails of mixed lamellar structure crystallized developing the sub-α phase that gives origin to the second observed exothermic peak. If the melting curve is taken into account, the above cited mesophases melted at 65.02 ± 0.43°C and 16.64 ± 0.31°C and a further endothermic peak appeared at high temperature (68.91 ± 0.15°C), probably indicating the presence of a more

243 stable polymorph (β' or β). The enthalpy of melting, corresponding to the twin peaks at high
244 temperature, is approximately 87.0±0.5 J/g.

245 A similar trend, i.e. two peaks at high and low temperature was found for the organogels. The
246 high temperature peak moves towards lower temperature with increasing Myverol concentration
247 and it appears at the same temperature at which a sudden increase in the complex modulus was
248 found, indicating the beginning of crystallization (T_{co}). Therefore, it seems reasonable to assume
249 that the first transition peak corresponds to the self-assemble of the organogelator into the inverse
250 lamellar phase as a precursor of crystal growth and aggregation. The second transition peak
251 appears for all samples at approximately 15°C (very close to the sub-α transition temperature of
252 pure MAGs) and was found to be independent on the organogelator concentration. This low-
253 temperature peak (corresponding to a moderate change in the slope of the complex modulus curve
254 in Fig. 1) indicates the polymorphic transition into a crystalline form, analogous to the sub-α
255 crystals observed for pure MAGs. These results are in agreement with previous data by Chen et
256 al. [26] who observed a similar behavior for monostearin/hazelnut oil organogels. At higher
257 temperature, samples containing low amount of MAGs ($VM_{0.015}$ and $VM_{0.034}$) show a single broad
258 peak, whereas two consecutive endotherms can be observed for higher MAG concentration
259 ($VM_{0.300}$) and the pure organogelator, indicating the melting of two different structures. According
260 to Ojijo et al. [31], high MAG concentrations result in high degree of supersaturation and, thus,
261 crystal nucleation may occur in both α and β polymorphs, which explains the presence of the twin
262 peak.

263 The DSC analysis for VP samples with X_P = 0.010, 0.050, and 0.300 is shown in Fig. 3b. The
264 thermogram of pure policosanol exhibited two exothermic peaks upon cooling. In agreement with
265 literature [43] exothermic peaks appeared at 80.14 ± 0.21°C and 58.23 ± 0.18°C, whereas melting
266 peaks were observed at 59.45 ± 0.27°C and 81.49±0.17°C, associated with the potential presence
267 of α and γ typical polymorphs of fatty alcohols [44]. The enthalpy of crystallization and melting
268 are 167 ± 1 J/g and 159 ± 0.8 J/g, respectively. As far as the other samples are concerned, the

three cooling and melting curves exhibited clearly different behavior. The crystallization of $VP_{0.010}$ sample (X_P = 0.01) showed one small exothermic peak and a small endothermic peak during melting. The transition peak observed upon cooling appeared at the same temperature at which of the sharp increase in G^* curve evidenced the beginning of crystallization (T_{co}).

The thermogram of sample $VP_{0.050}$ exhibited only one exothermic twin peak during cooling and one broad peak upon heating. A behavior similar to 3% w/w Candelilla wax in safflower oil organogel as investigated by Toro-Vazquez et al. [39]: here the peak in both the cooling and heating thermograms was associated with the gelation and melting of Candellilla wax components mainly hentriacontane. Similarly, the twin peak observed in $VP_{0.050}$ cooling thermogram could be related to the crystallization of policosanol components, especially octacosanol ($C_{28}H_{58}O$). The behavior of $VP_{0.300}$ sample was found to be more complex in comparison to other samples. A narrow exothermic peak can be observed at high temperature in the cooling thermogram followed by a smaller twin peak, whereas the melting thermogram evidenced first a narrow peak followed by a broad endothermic peak. The DSC thermogram of $VP_{0.300}$ sample was found to be qualitatively very similar to that of C_{32}-alkane (dotriacontane, $C_{32}H_{66}$) reported by Morales-Rueda et al. [45]. The two exothermic peaks in the dotriacontane thermogram were associated with the development of a rotator phase from the melt and the transition from the rotator phase to crystal, while the first endothermic peak in the melting region was associated with a solid-solid transition from the crystalline to the rotator phase and the second peak to the transition from the rotator to the liquid phase [45, 46]. In addition, Morales-Rueda et al. [45] investigated a dispersion of 3% w/w C_{32} in safflower oil, obtaining results similar to those found in this work for organogels prepared with low policosanol fractions. Therefore, it suggested that at high organogelator fractions the thermal behavior of organogels is mainly due to the longest-chain components of policosanol, whereas at low policosanol fractions a less complex behavior is observed.

3.1.3 FT-IR analysis

FT-IR spectra are recorded at room temperature immediately after gel formation. The high-energy region from 3000 to 4000 cm^{-1} is particularly interesting because it corresponds to the OH-stretching modes [22]. Monoglycerides have two OH groups in the hydrophilic part of the molecule with 3-OH the most external group and 2-OH in a more buried configuration. The hydrogen bonds formed by each hydroxyl group can be detected by the peaks appearing at different wavenumbers. Fig. 4a shows spectra recorded for samples $VM_{0.015}$, $VM_{0.034}$, and $VM_{0.300}$. In the low-energy region, a small inflection can be detected in $VM_{0.015}$ spectrum, whereas a broad peak appears in $VM_{0.034}$ and a twin peak in $VM_{0.300}$ spectra. The single peak occurring for $VM_{0.034}$ sample between 3000 and 3500 cm^{-1}, corresponds to 3-OH groups bonded with hydrogen bonds [22], while the high-energy twin peak of $VM_{0.300}$, detectable in the same wavenumbers region, corresponds to both 3-OH and 2-OH hydrogen bonding [22]. The coexistence of 3-OH and 2-OH hydrogen bonding was already observed by Chen and Terentjev [22] during aging of MAG/hazelnut oil organogels. They associated the presence of 2-OH hydrogen bonding to the formation of the stable β crystal polymorph. The obtained results suggest the formation of an inverse lamellar phase in $VM_{0.034}$ system and the coexistence of lamellar structures and β crystals in $VM_{0.300}$ system. This is in agreement with results obtained from DSC analysis as discussed above.

Of course also other intermolecular interactions could be responsible for organogel formation such as van der Waals forces [17, 18], especially for long alkyl chains organogelators. Suzuki et al. [47] showed that van der Waals interactions shifted the absorption bands of symmetric and anti-symmetric CH_2 stretching vibrational modes to lower wavenumbers. As a consequence, with the aim of investigating the potential presence of additional interactions, the position of absorption bands of CH_2 stretching were determined for investigated organogels. They were observed at 2922 cm^{-1} and 2853 cm^{-1} for sample $VM_{0.015}$, where gelation does not occur, whereas they were found at 2920 cm^{-1} and 2852 cm^{-1} as well as at 2920 cm^{-1} and 2850 cm^{-1} for samples $VM_{0.034}$ and $VM_{0.3}$, respectively. Although differences between these values are small, the wavenumber shift

could be attributed to a decrease in the fluidity of the alkyl chains, suggesting the presence of van der Waals interactions [47]. Even at high MAGs concentration, i.e. x_M=0.300, the shift is quite small and approximately similar to those found at lower concentration, whereas the peak corresponding to H bonding increases (and a twin peaks appears at high concentration). This could suggest that even if both interactions are present, the H bonding is more relevant in gel formation.

Following the analysis carried out for MAGs organogels, Fig. 4b shows the FT-IR results for samples $VP_{0.003}$, $VP_{0.050}$, and $VP_{0.300}$. Sample $VP_{0.003}$ and $VP_{0.050}$ spectra did not show the presence of any intermolecular hydrogen bonds. For $VP_{0.003}$ this might be due to the low organogelator concentration, but also for sample $VP_{0.050}$ produced well above the minimum policosanol concentration required for gelation, no intermolecular hydrogen bonding was detected. Sample $VP_{0.300}$ exhibited a different behavior, with a small peak at around 3300 cm^{-1}. This peak can be associated with the presence of weak intermolecular hydrogen bonds [48]. Thus only at high organogelator concentrations, the formation of hydrogen bonds as interactions among policosanol molecule aggregates can be observed. Therefore it can generally be concluded that the presence of hydrogen bonds was not the main "driving force" for policosanol organogel formation. When the absorption bands of symmetric and anti-symmetric CH_2 stretching vibrational modes are considered, changes are observed; for sample $VP_{0.003}$ (no gel formation within the investigated temperature range, according to rheological results) the above-mentioned bands appeared at 2922 cm^{-1} and 2853 cm^{-1}, whereas for sample $VP_{0.050}$ peaks were observed at 2920 cm^{-1} and 2851 cm^{-1} and for sample $VP_{0.300}$ at 2917 cm^{-1} and 2848 cm^{-1}. As already discussed, the wavenumber shift can be attributed to the organization of the alkyl groups via van der Waals interactions [47].

In summary, both hydrogen bonding and van der Waals interactions seem to be present in both systems, even if the specific contributions to the final organogel are quite different. MAGs organogel formation is highly dependent on the formation of hydrogen bonds between organogelator molecules, owing to the presence of two OH groups that are responsible of the hydrogen interactions, increasing with increasing amount of gelator. On the other hand, van der

346 Waals interactions seem less relevant and almost constant with gelator amount, at least, up to
347 X_M=0.300.

348 The long alkyl chains, in policosanol, are able to create significant nonspecific interactions that
349 yield the network formation in organogels mainly through van der Waals interactions, whereas
350 H-bonding, related to a single OH group, seems to be present only at high policosanol fractions.

351 The different contributions of van der Waals interactions can be explained, first of all, considering
352 the different length of the alkyl chains, in agreement with literature results obtained for different
353 gelators of the same family with a different number of methylene units [49]. Moreover, in the
354 same work [49], a lower contribution of van der Waals interactions was observed in systems
355 where gelator was more soluble, as an effect of the improved solvation. It is worth mentioning
356 that MAGs are more soluble than policosanol in virgin olive oil (see section 3.1.4) and therefore
357 it can be speculated that also the favorable solvation of MAGs reduces the contribution of van der
358 Waals gelator-gelator forces. Thus, gelation in MAGs can be mainly attributed to hydrogen
359 bonding, whereas in policosanol van der Waals interactions play the most important role and,
360 even though they are much weaker than hydrogen bonding [18], the length of the alkyl chain
361 seems sufficient to promote quite strong interactions.

362 These differences in intermolecular interactions could be partially responsible of the different
363 gelation ability of the investigated components: in fact, it was observed that, at the same
364 concentration, policosanol is able to gel the oil at higher temperatures than MAGs yielding
365 stronger gels. Suzuki et al. [50], in their work, attributed to the increasing van der Waals
366 interactions the growing ability of gelators with increasing alkyl chain length, to gel oil even at
367 high temperature. Therefore it could be speculated that a large number of van der Waals
368 interactions, among long alkyl chains of policosanol (mainly made of C_{28} molecules), could
369 promote the formation of gels stronger than those obtained by the MAGs chain (C_{16}-C_{18}) even
370 though stronger hydrogen interactions are present in this case. The results on the gel strength are
371 in agreement with values of melting temperature and enthalpy estimated for the organogelators:

372 DSC data evidenced that MAGs exhibit values lower than those observed for policosanol (see
373 Section 3.1.2) suggesting the presence of weaker gelator-gelator interactions as indicated by
374 Zweep et al .[49]

375 *3.1.4 Microstructure and macroscopic properties: the fractal model*

376 The SFC of both VM and VP systems was evaluated during cooling of sample. An increase with
377 decreasing temperature with a similar trend to G^* during temperature ramp tests is observed (see
378 Fig. S1 in Supplementary Material). At high temperature ($T > T_{co,NMR}$) the SFC is almost zero. At
379 the onset of crystallization ($T = T_{co,NMR}$) a sharp growth of the SFC can be detected, followed by
380 a transition region and finally a plateau, very close to the mass fraction of the organogelator of
381 the system can be observed at $T < T_{co,NMR}$.

382 If the SFC of organogelators is determined and used to compute a "theoretical SFC" [51], it can
383 be seen that theoretical values are slightly higher than experimental ones, as already reported in
384 the literature for Myverol [52] Observed differences are generally larger for policosanol than for
385 Myverol. The lower policosanol solubility with respect to Myverol suggest the presence of lower
386 solvent-gelator interactions which promote policosanol separation and aggregation at
387 temperatures higher than those observed for Myverol explaining the higher T_{co} observed for
388 policosanol

389 In the present work, the fractal model proposed by Tang and Marangoni [53] has been used to
390 relate the rheological properties of organogels to their microstructure [29]. The non-linear
391 relationship between storage modulus G' and the volumetric fraction of solids Φ in fat crystal
392 networks can be expressed as follows:

393 $$G' = \lambda \Phi^{\frac{1}{3-D}} \quad (4)$$

394 where λ is a constant depending on the strength of the interactions between fat crystal flocs and
395 D is the fractal dimension of the network. To describe the material behavior in a wide range of

solid fraction the apparent solid volume fraction Φ has to be replaced with the effective volume fraction Φ_e of stress-loading solids yielding the so-called "modified fractal model" [54]:

$$G' = \lambda\left(1 - e^{-k\Phi^b}\right)^{\frac{1}{3-D}} \quad (5)$$

Due to the limited number of experimental available data it was not possible to directly fit data to Eq. (5). As a consequence, the fractal dimension D was first estimated in a limited range of volume fractions using Eq. (4) and it was obtained 2.74 ± 0.02 and 2.78 ± 0.01 for VM and VP samples, respectively. Then Eq. (5) was used with the computed D value to fit experimental data on the whole concentration range. In the case of VM, the modified fractal model fits the experimental data at intermediate and high volume fractions of organogelators well (Fig. 5). In the case of VP samples, a lower number of experimental points were available and, therefore, only Eq. (4) was used also providing reasonable fitting as shown in Fig. 5.

Even if different interactions are the main responsible for network formation, the macroscopic fractal dimension is approximately the same. Moreover the estimated values of D are in good agreement with typical values obtained in the literature [54, 55] for colloidal networks of fat crystals (2.82 - 2.89 for palm oil, 2.37 - 2.46 for cocoa butter, and 2.81 for anhydrous milk fats) or for olive oil/monoglyceride organogels (2.79 computed by data shown by Ojijo et al, [31] for a different form of the fractal model).

3.2 Effects of organogelators on gels based on different oils

3.2.1 Rheological characterization

The effects of the vegetable oil used as the solvent were investigated for samples prepared at a constant organogelator fraction (X = 0.03 for samples EM, $VM_{0.030}$, and SM with Myverol and EP, $VP_{0.030}$, and SP with policosanol). During temperature ramp tests, complex modulus and phase angle curves showed the same behavior already described. In general, T_{co} is independent of oil

composition, as already shown in the literature for MAGs content larger than 3% (w/w) and with faster cooling rate (-5°C/min) [30]. However, it can be observed that the gelation temperature T_g of $VM_{0.030}$ is lower than the value exhibited by EM and SM samples, whereas no difference can be detected for the gelation temperatures of samples EP, SP, and $VP_{0.030}$. This result is in agreement with *SDr* data (see Fig. 2): a slower gelation for $VP_{0.030}$ with respect to EP and SP is observed and, therefore a lower gelation temperature is obtained. On the other hand policosanol gels exhibits the same *SDr* value independent of the oil, and as a consequence, the gelation temperature is the same for all investigated oils.

The potential influence of the oil on the final consistency of the organogel was analyzed also comparing G^* at temperatures below T_{co} (T_5, T_{10}, T_{15}, and T_{25}, see Fig. 1). For MAGs samples (Fig. 6) no relevant difference can be found between EM and $VM_{0.030}$ in the entire temperature range, whereas samples prepared with sunflower oil or with olive oil differ in a narrow range close to the crystallization onset. In the case of VP samples, no significant difference was detected upon cooling for the three considered samples. This is in agreement with results reported by Gandolfo et al. [37] showing that the kind of oil had no significant effect on the rheological properties of fatty alcohol organogels.

3.2.2 FT-IR analysis

The effect of different oils on intermolecular interactions and on gelation rate was investigated also by performing FT-IR tests at two different storage times. When samples prepared with Myverol are studied immediately after their preparation (Fig. 7a), for the same gelator fraction, i.e. X_M=0.03, the twin peak showing the presence of both 3-OH and 2-OH hydrogen bonding [22] is more evident in EM and SM samples, with respect to $VM_{0.030}$. These results seem to suggest, apparently, that the "intensity" of hydrogen bonding, at constant gelator amount, could depend on the solvent source. On the other hand, when samples stored for one week at +25°C were also studied no difference among the samples was observed (Fig. 7b) and the same peaks were identified in all cases.

446 As a consequence, it can be speculated that apparent differences, observed in samples
447 immediately after preparation, are only due to kinetic effects: hydrogen bonds among molecules
448 are slowly formed in V oil, yielding only a small inflections in FT-IR tests: this causes a slow
449 *SDr* and low gelation temperature, as observed in rheological tests. Anyway, after an annealing
450 period, these differences disappear. On the other hand, the same bonding is faster in E and S, as
451 suggested also by rheological *SDr*, and the peaks related to hydrogen interactions are evident
452 immediately after sample preparation and they do not change after the annealing period.

453 The different behavior observed between V and E is quite unexpected because their composition,
454 in terms of fatty acids, is similar and main differences, between them, are related to potential
455 impurities and to free acid content [56]. The free acid content in S (in terms of equivalent oleic
456 acid) is lower than 0.3 g/100 g, whereas, the limit in free acid content is 0.8 g/100 g for extra-
457 virgin olive oil and 2 g/100 g for virgin oil [56]. It is evident that V oil is characterized by a
458 content quite higher with respect to the other oils: it could be supposed that the larger amount of
459 free acids strengthen the solvent-gelator interactions hindering the formation of the gelator-
460 gelator bonding and delaying the gelation phenomena.

461 On the other hand, FT-IR spectra of all policosanol samples showed, in all solvents, the absence
462 of hydrogen bonding, confirming that gelation is mainly due to van der Waals interactions (data
463 not shown). The FT-IR results also explain the *SDr* values (Fig. 2) obtained for policosanol
464 organogels that are constant and, usually, lower than those observed for Myverol gels: van der
465 Waals interactions are much weaker than H-bonding and, thus, gelation based on the latter is
466 usually faster than that observed when only van der Waals interactions are present [18]. Moreover,
467 being van der Waals interactions nonspecific, the same organogel structure and therefore the same
468 *SDr* are observed in all oils. Only in V policosanol gelation is faster than MAGs one, owing to
469 the already discussed phenomena.

470 *3.2.3 Rheo-optical analysis*

In order to observe the network structure of organogels produced with different vegetable oils during rheological measurements a rheo-optical module during temperature ramp tests was utilized.

For all samples containing Myverol (Fig. 8a and Fig. S1-S2 in supplementary material), only small crystal nuclei can be observed at T = T_{co}. At lower temperatures, images show crystals with needle-like shape, similar to those observed by Kesselman and Shimoni [28] for MAG/olive oil oleogels and by López-Martínez et al. [41] for MAG/safflower oil organogels. For olive oils (both V and E) at T ≤ T_g crystals seem to yield quite long fibers aggregating in structure where they are oriented in the same direction (like bundle of fibers). On the other hand, in S, shorter fibers aggregating in structure more similar to flocs can be observed. Anyway, it seems that these small differences in the crystalline structure do not yield appreciable differences in rheological behavior. A comparison among the results obtained for samples produced with policosanol and three different solvents (see Fig. 8b and Fig S3-S4 in supplementary material), shows that the crystallization is quite fast. For all tested samples, the dimensions of the needle-like crystals is apparently unaffected by the solvent, which is in agreement with the previous discussion on policosanol behavior.

Finally, a comparison between the crystals produced with MAGs and policosanol (see for example Fig. 8a and 8b) indicates that fatty alcohols produce, generally speaking, fibers longer than those produced by monoglycerides, which can explain the different rheological behavior of VM and VP and is probably due to the different interactions among gelators molecules.

4. CONCLUSIONS

493 The present paper investigated the relationship between macroscopic properties and
494 microstructure of edible organogels based on two different low molecular weight organogelators,
495 i.e. monoglycerides of fatty acids (MAGs) and policosanol.

496 The material characterization was carried out by using NMR, rheology and DSC, whereas FT-IR
497 spectroscopy was used to investigate the intermolecular interactions driving the organogel
498 formation. Previous studies on intermolecular interactions in organogels were mainly carried out
499 on non-edible organic solvents [22, 47, 57], while only a few investigations employ FT-IR
500 combined with other techniques to investigate hydrogen bonding and van der Waals interactions
501 in edible systems.

502 The onset of crystallization (T_{co}) was determined by using NMR, rheology, and DSC and no
503 significant differences were found among the applied techniques in agreement with literature data
504 obtained by using different rheological methods [30]. DSC cooling tests showed at temperature
505 lower than T_{co}, transitions in crystalline structures for both MAGs and policosanol, only at high
506 concentration for the latter. Results obtained for MAGs are similar to previous literature data on
507 different organogels [26]. Rheology was less sensitive in detecting polymorphic transitions
508 whereas it was very powerful in evidencing the formation of a network and, therefore, the gelation
509 of the material. The investigation identified a number of significant differences in intermolecular
510 interactions between policosanol and MAGs. FT-IR measurements showed that MAGs gelation
511 is mainly due to H-bonding whereas van der Waals forces seem less relevant also at high gelator
512 fractions. On the other hand in policosanol mainly van der Waals interactions are present and H-
513 bonding appears only at high organogelator fractions. Because of these different interactions,
514 MAGs gelation occurs faster than policosanol one, as seen in the rheological *SDr* data and it can
515 be a function of the oil. In virgin olive oil *SDr* is different with respect to other oils, because of
516 the different content in free fatty acids affecting the hydrogen interactions. On the contrary, van
517 der Waals interactions are less specific and no evident differences in gelation rate were observed
518 in investigated oils. Typically, the gelation occurs at a slower way, because of the weaker energy

519 of the van der Waals interactions compared to H-bonding [18]. Despite this, policosanol gels are
520 stronger than MAGs ones and are obtained at lower concentration: this could be due to the large
521 number of interactions that are formed among the long chains of fatty alcohols. As a consequence,
522 rheological properties such as complex modulus and phase angle depend on both organogelators
523 and oil composition. Differences were observed between sunflower oil and olive oil (both virgin
524 and extra virgin) samples, even though they become quite small at low temperature. These oils
525 differ mainly in fatty acids profile being the sunflower oil richer in polyunsaturated fatty acids
526 than the olive ones [58]. SFC determination showed a lower solubility of policosanol in olive oil,
527 with respect to Myverol and, thus, suggesting the presence of lower solvent-gelator interactions
528 which probably promote policosanol separation and aggregation at temperatures higher than that
529 observed for Myverol. This effect seems independent of adopted solvent and therefore the onset
530 of crystallization was found function only of the nature and amount of gelator.

531 Finally, a rheo-optical approach carried out during temperature ramp tests showed the formation
532 of fiber-like structures. Different apparent length could be observed for MAGs (shorter fibers)
533 and policosanol (longer fibers). Moreover, the different oils seem to modify the shape and the
534 packing level of the obtained aggregates yielding to the slight differences observed during
535 rheological tests. The structural study carried out in this work suggests that policosanol is very
536 effective in organogelation and seems very promising for uses in food and nutraceutical area,
537 being itself a nutraceutical component and being less sensitive to the adopted solvent. Future
538 works should further investigate the intermolecular interactions in policosanol system and the
539 organogel properties with different solvents (both for edible and cosmetic uses) having different
540 polarity to confirm the “flexibility” of this organogelator.

REFERENCES

[1] N. Siraj, M.A. Shabbir, T. Ahmad, A. Sajjad, M.R. Khan, M.I. Khan, M.S. Butt, Organogelators as a Saturated Fat Replacer for Structuring Edible Oils, International Journal of Food Properties 18(9) (2015) 1973-1989.

[2] F.R. Lupi, D. Gabriele, B. de Cindio, M.C. Sanchez, C. Gallegos, A rheological analysis of structured water-in-olive oil emulsions, Journal of Food Engineering 107(3-4) (2011) 296-303.

[3] E.D. Co, A.G. Marangoni, Organogels: An Alternative Edible Oil-Structuring Method, Journal of the American Oil Chemists Society 89(5) (2012) 749-780.

[4] F.R. Lupi, L. Gentile, D. Gabriele, S. Mazzulla, N. Baldino, B. de Cindio, Olive oil and hyperthermal water bigels for cosmetic uses, Journal of Colloid and Interface Science 459 (2015) 70-78.

[5] A.K. Zetzl, A.G. Marangoni, S. Barbut, Mechanical properties of ethylcellulose oleogels and their potential for saturated fat reduction in frankfurters, Food & Function 3(3) (2012) 327-337.

[6] F.R. Lupi, D. Gabriele, L. Seta, N. Baldino, B. de Cindio, Rheological design of stabilized meat sauces for industrial uses, European Journal of Lipid Science and Technology 116(12) (2014) 1734-1744.

[7] F.R. Lupi, D. Gabriele, N. Baldino, L. Seta, B. de Cindio, C. De Rose, Stabilization of meat suspensions by organogelation: A rheological approach, European Journal of Lipid Science and Technology 114(12) (2012) 1381-1389.

[8] J.F. Toro-Vazquez, R. Mauricio-Perez, M.M. Gonzalez-Chavez, M. Sanchez-Becerril, J.D. Ornelas-Paz, J.D. Perez-Martinez, Physical properties of organogels and water in oil emulsions structured by mixtures of candelilla wax and monoglycerides, Food Research International 54(2) (2013) 1360-1368.

[9] F.C. Wang, A.J. Gravelle, A.I. Blake, A.G. Marangoni, Novel trans fat replacement strategies, Current Opinion in Food Science 7 (2016) 27-34.

[10] A.R. Patel, K. Dewettinck, Edible oil structuring: an overview and recent updates, Food & Function 7(1) (2016) 20-29.

[11] F.R. Lupi, D. Gabriele, N. Baldino, P. Mijovic, O.I. Parisi, F. Puoci, Olive oil/policosanol organogels for nutraceutical and drug delivery purposes, Food & Function 4(10) (2013) 1512-1520.

[12] S.S. Sagiri, B. Behera, R.R. Rafanan, C. Bhattacharya, K. Pal, I. Banerjee, D. Rousseau, Organogels as Matrices for Controlled Drug Delivery: A Review on the Current State, Soft Materials 12(1) (2013) 47-72.

[13] S.S. Sagiri, J. Sethy, K. Pal, I. Banerjee, K. Pramanik, T.K. Maiti, Encapsulation of vegetable organogels for controlled delivery applications, Designed Monomers and Polymers 16(4) (2013) 366-376.

[14] R. Sanz, A.C. Calpena, M. Mallandrich, B. Clares, Enhancing topical analgesic administration: Review and prospect for transdermal and transbuccal drug delivery systems, Current Pharmaceutical Design 21(20) (2015) 2867-2882.

[15] K. Rehman, M.H. Zulfakar, Recent advances in gel technologies for topical and transdermal drug delivery, Drug Development and Industrial Pharmacy 40(4) (2014) 433-440.

[16] D.J. Abdallah, R.G. Weiss, n-alkanes gel n-alkanes (and many other organic liquids), Langmuir 16(2) (2000) 352-355.

[17] J.H. van Esch, B.L. Feringa, New Functional Materials Based on Self-Assembling Organogels: From Serendipity towards Design, Angewandte Chemie International Edition 39(13) (2000) 2263-2266.

[18] Y. Wu, S. Wu, G. Zou, Q. Zhang, Solvent effects on structure, photoresponse and speed of gelation of a dicholesterol-linked azobenzene organogel, Soft Matter 7(19) (2011) 9177-9183.

[19] G. Zhu, J.S. Dordick, Solvent Effect on Organogel Formation by Low Molecular Weight Molecules, Chemistry of Materials 18(25) (2006) 5988-5995.

592 [20] R. Luboradzki, O. Gronwald, M. Ikeda, S. Shinkai, D.N. Reinhoudt, An Attempt to Predict
593 the Gelation Ability of Hydrogen-bond-based Gelators Utilizing a Glycoside Library,
594 Tetrahedron 56(49) (2000) 9595-9599.

595 [21] M. Burkhardt, S. Kinzel, M. Gradzielski, Macroscopic properties and microstructure of HSA
596 based organogels: Sensitivity to polar additives, Journal of Colloid and Interface Science 331(2)
597 (2009) 514-521.

598 [22] C.H. Chen, E.M. Terentjev, Aging and Metastability of Monoglycerides in Hydrophobic
599 Solutions, Langmuir 25(12) (2009) 6717-6724.

600 [23] F. Valoppi, S. Calligaris, L. Barba, M.C. Nicoli, Structural and viscoelastic characterization
601 of ternary mixtures of sunflower oil, saturated monoglycerides and aqueous phases containing
602 different bases, Food Research International 74 (2015) 224-230.

603 [24] S. Calligaris, S. Da Pieve, G. Arrighetti, L. Barba, Effect of the structure of monoglyceride-
604 oil-water gels on aroma partition, Food Research International 43(3) (2010) 671-677.

605 [25] H.D. Batte, A.J. Wright, J.W. Rush, S.H.J. Idziak, A.G. Marangoni, Effect of processing
606 conditions on the structure of mono stearin-oil-water gels, Food Research International 40(8)
607 (2007) 982-988.

608 [26] C.H. Chen, I. Van Damme, E.M. Terentjev, Phase behavior of C18 monoglyceride in
609 hydrophobic solutions, Soft Matter 5(2) (2009) 432-439.

610 [27] S. Da Pieve, S. Calligaris, E. Co, M.C. Nicoli, A.G. Marangoni, Shear Nanostructuring of
611 Monoglyceride Organogels, Food Biophysics 5(3) (2010) 211-217.

612 [28] E. Kesselman, E. Shimoni, Imaging of oil/monoglyceride networks by polarizing near-field
613 scanning optical microscopy, Food Biophysics 2(2-3) (2007) 117-123.

614 [29] F.R. Lupi, D. Gabriele, V. Greco, N. Baldino, L. Seta, B. de Cindio, A rheological
615 characterisation of an olive oil/fatty alcohols organogel, Food Research International 51(2) (2013)
616 510-517.

617 [30] F.R. Lupi, D. Gabriele, D. Facciolo, N. Baldino, L. Seta, B. de Cindio, Effect of
618 organogelator and fat source on rheological properties of olive oil-based organogels, Food
619 Research International 46(1) (2012) 177-184.

620 [31] N.K. Ojijo, I. Neeman, S. Eger, E. Shimoni, Effects of monoglyceride content, cooling rate
621 and shear on the rheological properties of olive oil/monoglyceride gel networks, Journal of the
622 Science of Food and Agriculture 84(12) (2004) 1585-1593.

623 [32] F.R. Lupi, D. Gabriele, B. de Cindio, Effect of Shear Rate on Crystallisation Phenomena in
624 Olive Oil-Based Organogels, Food and Bioprocess Technology 5(7) (2012) 2880-2888.

625 [33] F.M. Alvarez-Mitre, J.F. Toro-Vázquez, M. Moscosa-Santillán, Shear rate and cooling
626 modeling for the study of candelilla wax organogels' rheological properties, Journal of Food
627 Engineering 119(3) (2013) 611-618.

628 [34] F.M. Alvarez-Mitre, J.A. Morales-Rueda, E. Dibildox-Alvarado, M.A. Charó-Alonso, J.F.
629 Toro-Vazquez, Shearing as a variable to engineer the rheology of candelilla wax organogels, Food
630 Research International 49(1) (2012) 580-587.

631 [35] M. Ogutcu, E. Yilmaz, Oleogels of virgin olive oil with carnauba wax and monoglyceride as
632 spreadable products, Grasas Y Aceites 65(3) (2014).

633 [36] H.M. Schaink, K.F. van Malssen, S. Morgado-Alves, D. Kalnin, E. van der Linden, Crystal
634 network for edible oil organogels: Possibilities and limitations of the fatty acid and fatty alcohol
635 systems, Food Research International 40(9) (2007) 1185-1193.

636 [37] F.G. Gandolfo, A. Bot, E. Floter, Structuring of edible oils by long-chain FA, fatty alcohols,
637 and their mixtures, Journal of the American Oil Chemists Society 81(1) (2004) 1-6.

638 [38] J.A. Lopes Da Silva, M.P. Goncalves, M.A. Rao, Kinetics and thermal behaviour of the
639 structure formation process in HMP/sucrose gelation, International Journal of Biological
640 Macromolecules 17 (1995) 25-32.

641 [39] J.F. Toro-Vazquez, J.A. Morales-Rueda, E. Dibildox-Alvarado, M. Charo-Alonso, M.
642 Alonzo-Macias, M.M. Gonzalez-Chavez, Thermal and textural properties of organogels

643 developed by candelilla wax in safflower oil, Journal of the American Oil Chemists Society
644 84(11) (2007) 989-1000.

645 [40] J.F. Toro-Vazquez, J. Morales-Rueda, V.A. Mallia, R.G. Weiss, Relationship Between
646 Molecular Structure and Thermo-mechanical Properties of Candelilla Wax and Amides Derived
647 from (R)-12-Hydroxystearic Acid as Gelators of Safflower Oil, Food Biophysics 5(3) (2010) 193-
648 202.

649 [41] A. López-Martínez, J.A. Morales-Rueda, E. Dibildox-Alvarado, M.A. Charó-Alonso, A.G.
650 Marangoni, J.F. Toro-Vazquez, Comparing the crystallization and rheological behavior of
651 organogels developed by pure and commercial monoglycerides in vegetable oil, Food Research
652 International 64 (2014) 946-957.

653 [42] J. Vereecken, W. Meeussen, I. Foubert, A. Lesaffer, J. Wouters, K. Dewettinck, Comparing
654 the crystallization and polymorphic behaviour of saturated and unsaturated monoglycerides, Food
655 Research International 42(10) (2009) 1415-1425.

656 [43] L. Martinez, E. Uribarri, A. Laguna, Characterization and compatibility studies between
657 policosanol, a new hypocholesterolemic drug, and tablet excipients using differential scanning
658 calorimetry (DSC), Archiv Der Pharmazie 332(12) (1999) 439-441.

659 [44] F.G. Gandolfo, A. Bot, E. Floter, Phase diagram of mixtures of stearic acid and stearyl
660 alcohol, Thermochimica Acta 404(1-2) (2003) 9-17.

661 [45] J.A. Morales-Rueda, E. Dibildox-Alvarado, M.A. Charó-Alonso, R.G. Weiss, J.F. Toro-
662 Vazquez, Thermo-mechanical properties of candelilla wax and dotriacontane organogels in
663 safflower oil, European Journal of Lipid Science and Technology 111(2) (2009) 207-215.

664 [46] N. Wentzel, S.T. Milner, Crystal and rotator phases of n-alkanes: A molecular dynamics
665 study, Journal of Chemical Physics 132(4) (2010) 10.

666 [47] M. Suzuki, Y. Nakajima, M. Yumoto, M. Kimura, H. Shirai, K. Hanabusa, Effects of
667 hydrogen bonding and van der Waals interactions on organogelation using designed low-
668 molecular-weight gelators and gel formation at room temperature, Langmuir 19(21) (2003) 8622-
669 8624.

[48] R.d. Adel, P.C.M. Heussen, A. Bot, Effect of water on self-assembled tubules in β-sitosterol + γ-oryzanol-based organogels, Journal of Physics Conference Series (Online) 247(1) (2010) 12.

[49] N. Zweep, A. Hopkinson, A. Meetsma, W.R. Browne, B.L. Feringa, J.H. van Esch, Balancing Hydrogen Bonding and van der Waals Interactions in Cyclohexane-Based Bisamide and Bisurea Organogelators, Langmuir 25(15) (2009) 8802-8809.

[50] M. Suzuki, T. Nigawara, M. Yumoto, M. Kimura, H. Shirai, K. Hanabusa, l-Lysine based gemini organogelators: their organogelation properties and thermally stable organogels, Organic & Biomolecular Chemistry 1(22) (2003) 4124-4131.

[51] A.I. Blake, E.D. Co, A.G. Marangoni, Structure and Physical Properties of Plant Wax Crystal Networks and Their Relationship to Oil Binding Capacity, Journal of the American Oil Chemists Society 91(6) (2014) 885-903.

[52] E. Tarabukina, F. Jego, J.M. Haudin, P. Navard, E. Peuvrel-Disdier, Effect of Shear on the Rheology and Crystallization of Palm Oil, Journal of Food Science 74(8) (2009) E405-E416.

[53] D. Tang, A.G. Marangoni, Modeling the rheological properties and structure of colloidal fat crystal networks, Trends in Food Science & Technology 18(9) (2007) 474-483.

[54] D. Tang, A.G. Marangoni, Modified fractal model and rheological properties of colloidal networks, Journal of Colloid and Interface Science 318(2) (2008) 202-209.

[55] S.S. Narine, A.G. Marangoni, Relating structure of fat crystal networks to mechanical properties: a review, Food Research International 32(4) (1999) 227-248.

[56] E.U. Commission, Commission Implementing Regulation (EU) No 1348/2013 of 16 December 2013, Official Journal of the European Union L338 (2013) 31-36.

[57] M. Suzuki, T. Abe, K. Hanabusa, Low-molecular-weight gelators based on N(alpha)-acetyl-N(epsilon)-dodecyl-L-lysine and their amphiphilic gelation properties, Journal of Colloid and Interface Science 341(1) (2010) 69-74.

694 [58] M. Monfreda, L. Gobbi, A. Grippa, Blends of olive oil and sunflower oil: Characterisation
695 and olive oil quantification using fatty acid composition and chemometric tools, Food Chemistry
696 134(4) (2012) 2283-2290.

697

698

699 **TABLES CAPTIONS**

700 Table 1 Samples Identification: M means Myverol and P policosanol. V is virgin olive oil, E is
701 extra-virgin olive oil, and S is sunflower oil. The grey background indicates samples without
702 significant difference ($p<0.01$) between T_{co} and T_g

703

704

FIGURES CAPTIONS

Figure 1 Temperature Ramp Test for Sample $VM_{0.034}$ in terms of G* (full symbols) and phase angle (empty symbols). Dotted lines evidence temperatures at a constant distance from T_{co}, i.e. T_5, T_{10}, T_{15} and T_{25}.

Figure 2 *SDr* values for organogels produced with V, E and S with 3 %(w/w) of monoglycerides and policosanol (samples EM, SM, $VM_{0.030}$, EP, SP, $VP_{0.030}$)

Figure 3 DSC thermogram of samples $VM_{0.015}$, $VM_{0.034}$, $VM_{0.300}$ and Myverol (a) and $VP_{0.010}$, $VP_{0.050}$, $VP_{0.300}$ and Policosanol (b).

Figure 4 FT-IR spectra for $VM_{0.015}$, $VM_{0.034}$ and $VM_{0.300}$ samples (a) and for $VP_{0.003}$, $VP_{0.050}$ and $VP_{0.300}$ samples (b).

Figure 5 Storage modulus of organogel at T_{10} as function of volume fraction. Experimental data (closed circles VM, open circles VP) and fitting lines (red and light blue dotted lines are Eq. (4) and Eq. (5) data fittings for VM samples, solid black line is Eq. (4) data fitting for VP samples)

Figure 6 Complex modulus G* at different temperature levels for EM, $VM_{0.030}$ and SM samples.

Figure 7 FT-IR spectra for sample EM, SM and $VM_{0.030}$ immediately after the preparation (a) and after 1 week storage (b). Dotted lines evidence the different peaks in $VM_{0.030}$ spectra.

Figure 8 Temperature ramp test for sample EM (a) and EP (b) in terms of G* (full symbols) and phase angle (white symbols). Dotted lines correspond to the different micrographs taken at T_{co}, T_5, T_{10}, T_{15} and T_{25}. Control bar in T_{co} micrograph is 50 μm.

Table 1

732

Samples ID	Gelator fraction (w/w)	T_{co} (°C)	$T_{co,\ DSC}$ (°C)	$T_{co,\ NMR}$ (°C)	T_g (°C)	$SFC_{th}/100$ (-)	$SFC_{T25}/100$ (-)
$VM_{0.001}$	0.001	10.8±0.1	-	-	75±2	-	-
$VM_{0.005}$	0.005	18.0±0.1	-	-	8.1±0.1	-	-
$VM_{0.010}$	0.010	27.7±0.5	-	28.1±0.2	10.9±0.1	-	-
$VM_{0.015}$	0.015	32.6±0.3	32.8±0.2	32.9±0.1	25.6±0.1	-	-
$VM_{0.030}$	0.030	42.8±0.3	42.4±0.1	42.0±0.4	29.80±0.02	0.0290	0.0267±0.0001
$VM_{0.034}$	0.034	43.7±0.1	43.7±0.3	44.0±0.1	42.64±0.02	0.0329	0.0319±0.0003
$VM_{0.100}$	0.100	55.2±0.1	-	55.5±0.4	53.75±0.02	0.0967	0.0901±0.0001
$VM_{0.300}$	0.300	61.8±0.1	61.7±0.2	61.7±0.4	59.46±0.03	0.2900	0.289±0.001
$VM_{0.500}$	0.500	61.1±0.2	-	61.6±0.3	59.61±0.04	0.4834	0.4808±0.0007
EM	0.030	42.8±0.2	41.7±0.1	41.6±0.2	33.4±0.3	-	-
SM	0.030	42.0±0.5	42.0±0.1	42.1±0.2	34.1±0.4	-	-
$VP_{0.001}$	0.001	21.7±0.9	-	-	-	-	-
$VP_{0.003}$	0.003	34.2±0.4	-	34.7±0.3	-	0.0029	0.0027±0.0001
$VP_{0.005}$	0.005	38.2±0.1	-	38.6±0.4	26±1	0.0049	0.0046±0.0011
$VP_{0.010}$	0.010	42.1±0.4	42.7±0.1	42.2±0.3	39.5±0.3	0.0097	0.0095±0.0001
$VP_{0.020}$	0.020	47.7±0.1	-	47.1±0.4	45.6±0.3	0.0196	0.0182±0.0001
$VP_{0.025}$	0.025	50.3±0.5	-	50.8±0.2	49.4±0.1	0.0243	0.0225±0.0001
$VP_{0.030}$	0.030	52.0±0.3	52.2±0.1	52.3±0.5	50±3	0.0292	0.0268±0.0001
$VP_{0.034}$	0.034	53.8±0.2	53.6±0.1	53.4±0.3	51.9±0.4	0.0331	0.0320±0.0001
$VP_{0.050}$	0.050	56.5±0.3	57.0±0.2	56.9±0.2	54±1	0.0487	0.0451±0.0001
$VP_{0.150}$	0.150	65.7±0.1	-	65.1±0.6	64.0±0.8	0.1460	0.1421±0.0004
$VP_{0.300}$	0.300	72.5±0.5	73.0±0.1	72.3±0.4	71.6±0.7	0.2921	0.290±0.001
$VP_{0.550}$	0.550	76.7±0.1	-	76.2±0.4	76.3±0.1	0.5354	0.524±0.001
EP	0.030	52.4±0.2	52.3±0.1	52.5±0.2	50.5±0.2	-	-
SP	0.030	52.7±0.3	52.4±0.1	52.9±0.3	50.8±0.4	-	-

Figure 1

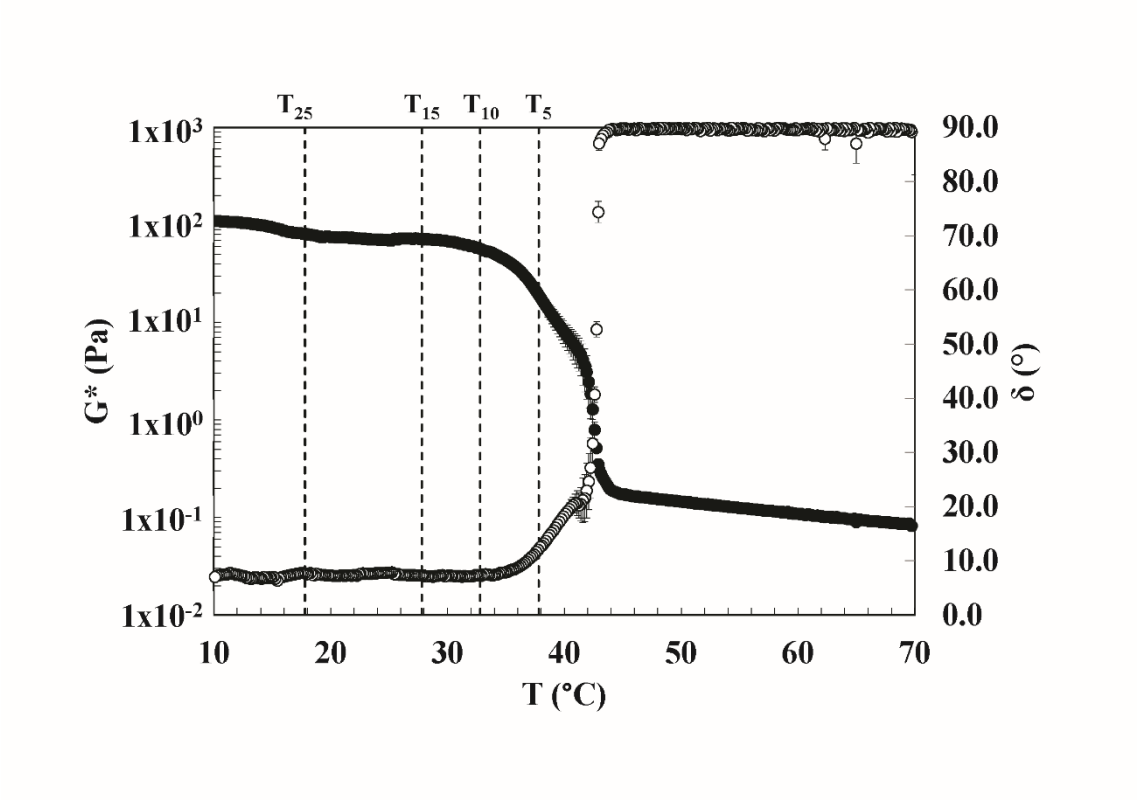
T25
T15
T10
T5
1x10^3
1x10^2
1x10^1
1x10^0
1x10^-1
1x10^-2
G* (Pa)
90.0
80.0
70.0
60.0
50.0
40.0
30.0
20.0
10.0
0.0
δ (°)
10
20
30
40
50
60
70
T (°C)

733

Figure 2

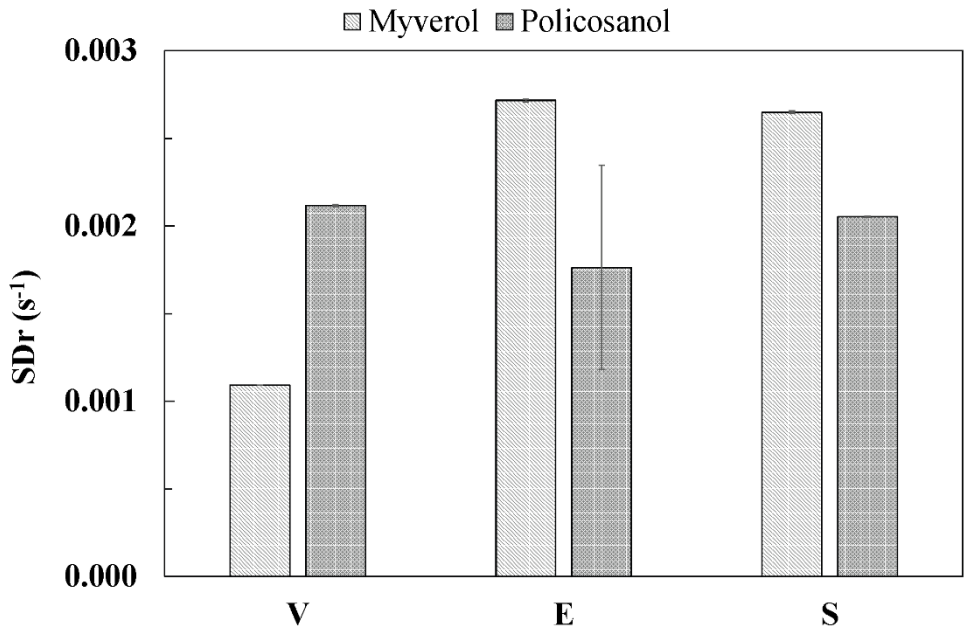

734

Figure 3a

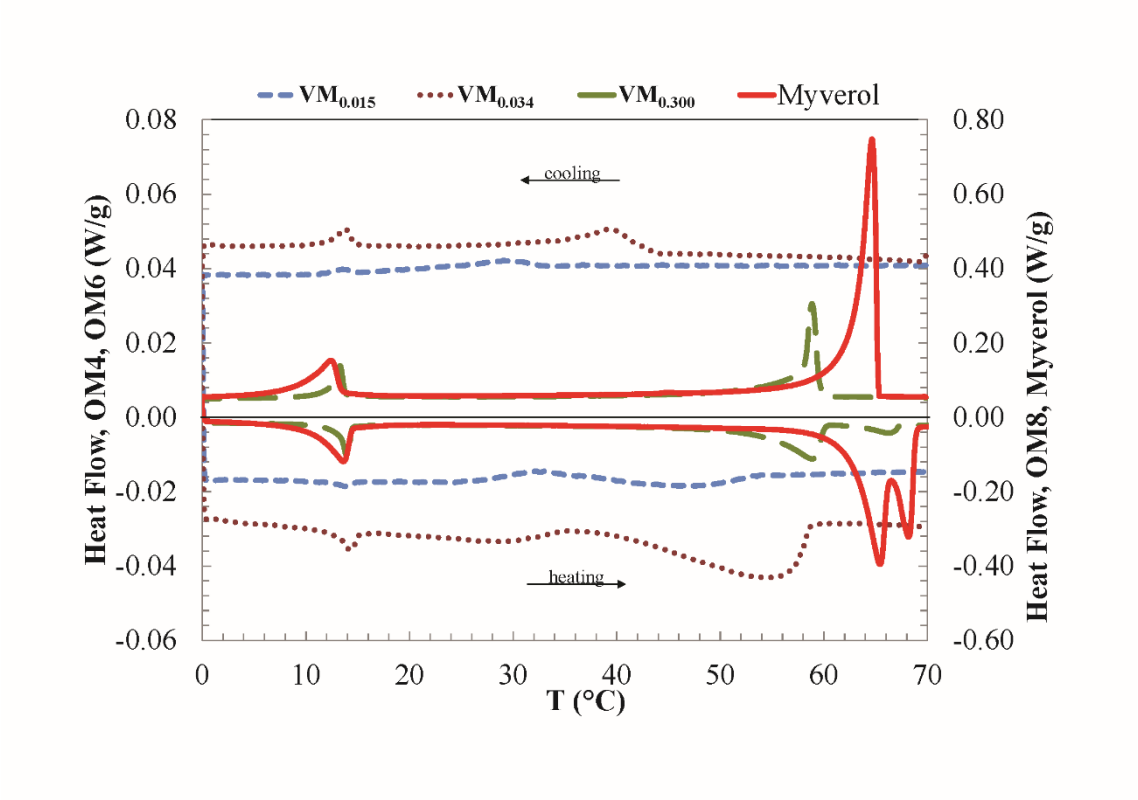

735

Figure 3b

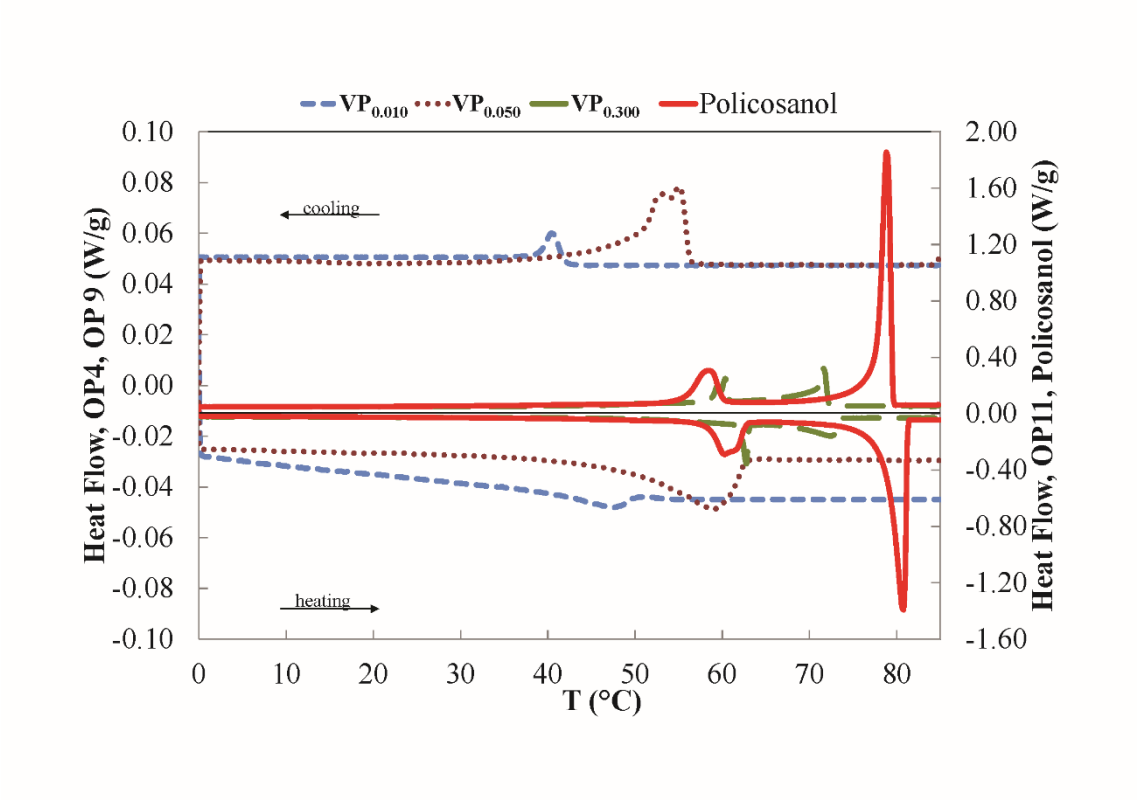

736

Figure 4

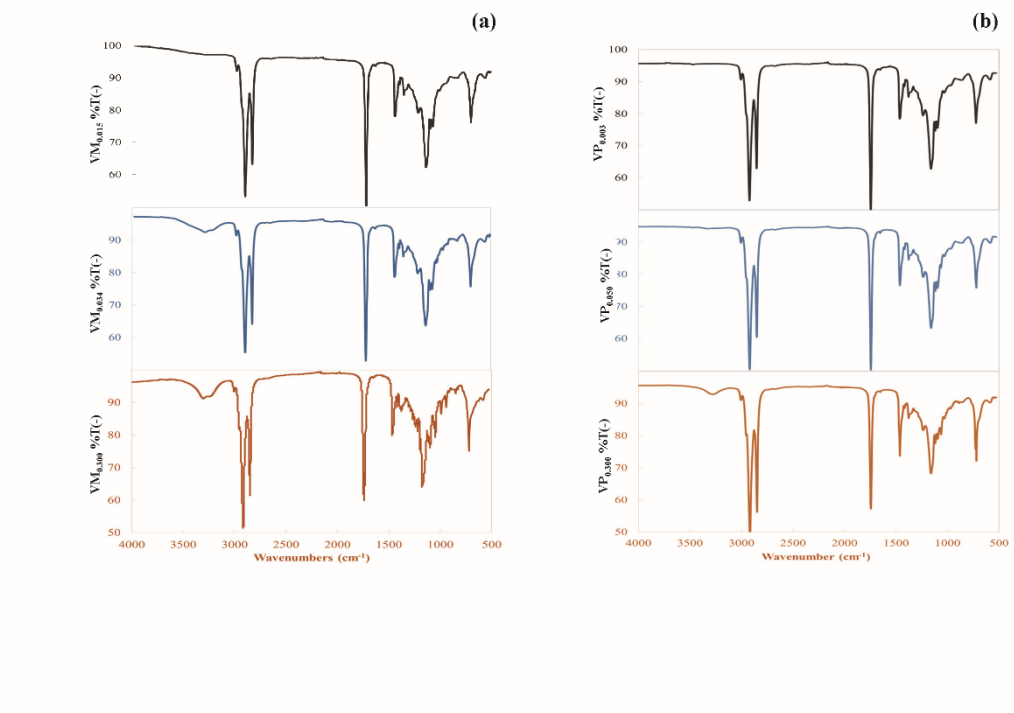

737

Figure 5

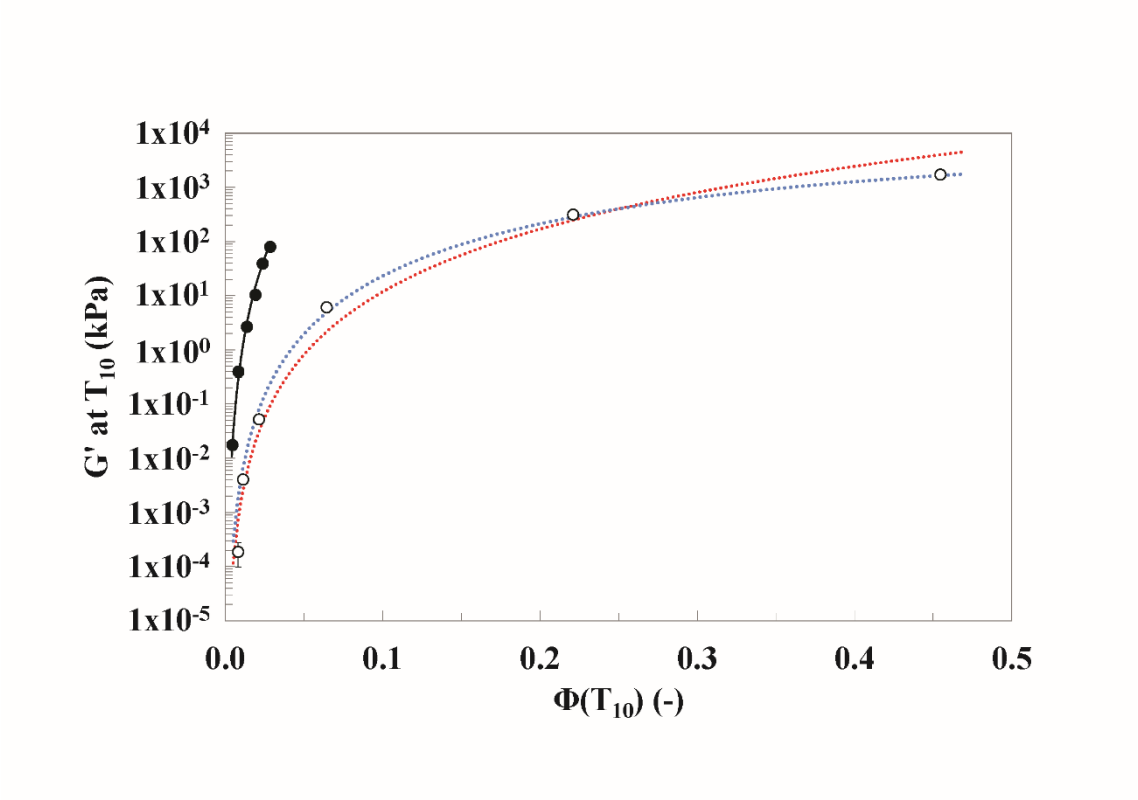
1x10^4
1x10^3
1x10^2
1x10^1
1x10^0
1x10^-1
1x10^-2
1x10^-3
1x10^-4
1x10^-5
G' at T10 (kPa)
0.0
0.1
0.2
0.3
0.4
0.5
Φ(T10) (-)

738

Figure 6

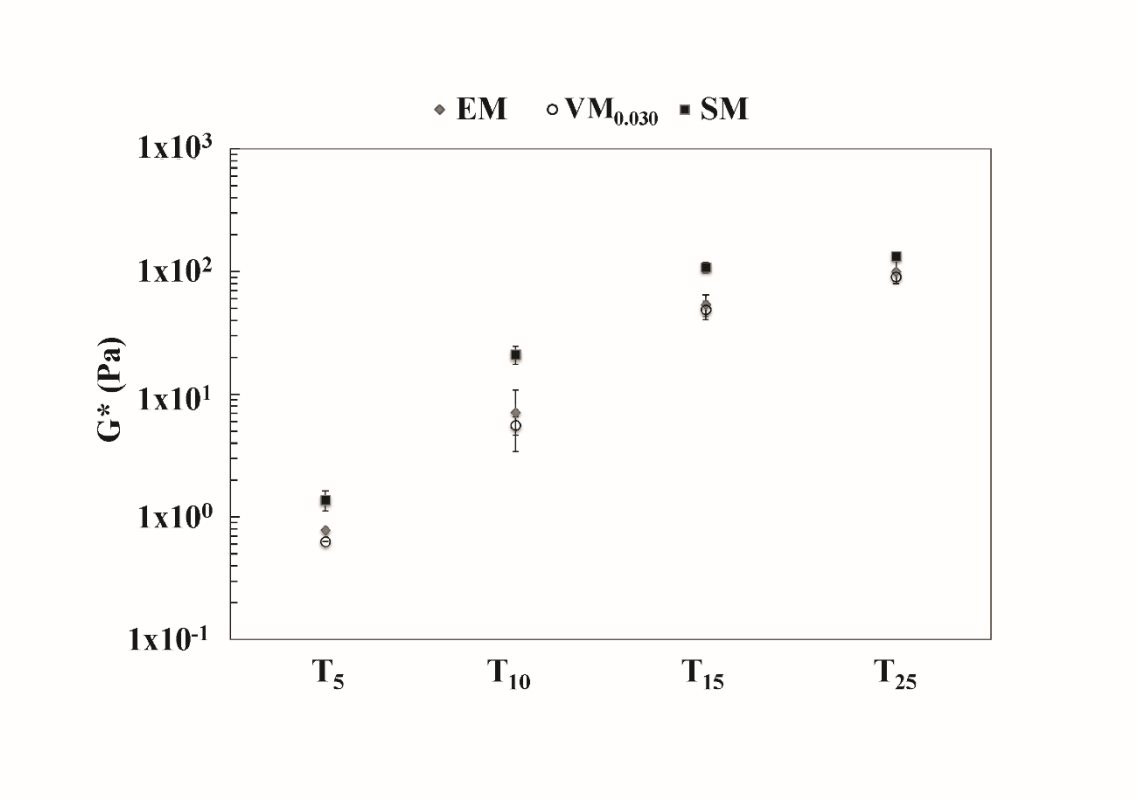

739

Figure 7

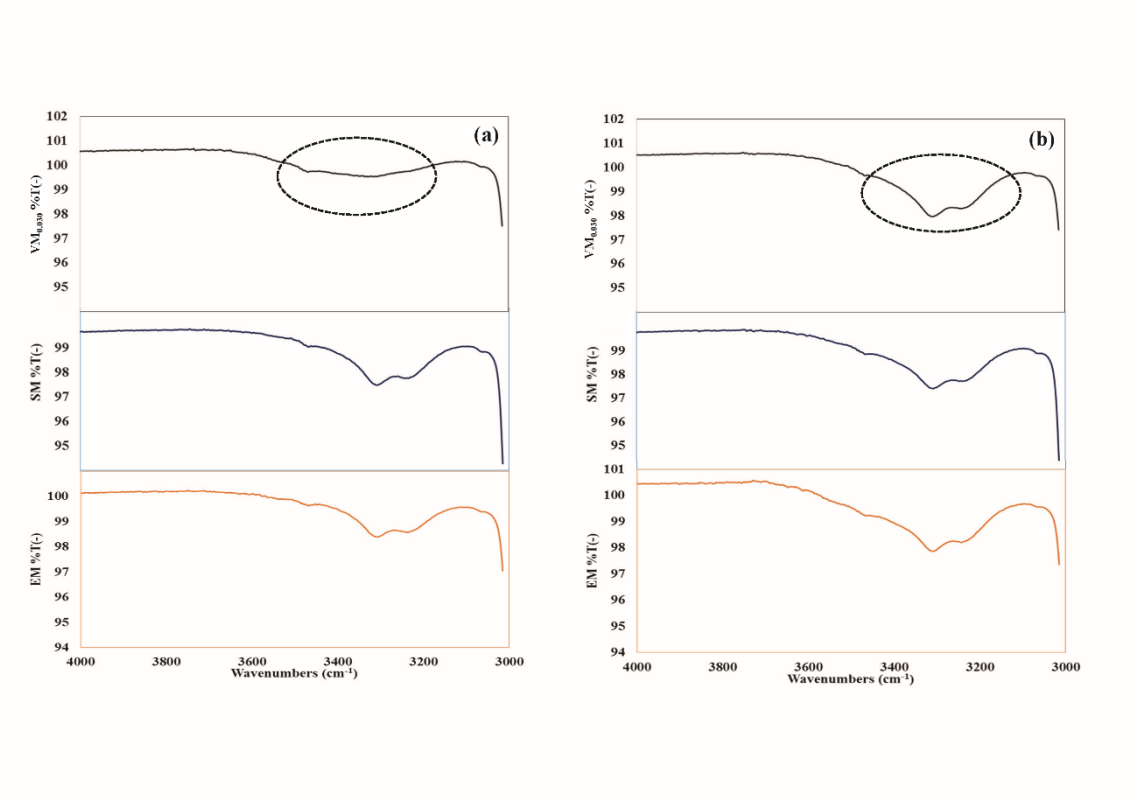
(a)
(b)
VM0.830 %T(-)
VM0.936 %T(-)
SM %T(-)
EM %T(-)
Wavenumbers (cm-1)
4000
3800
3600
3400
3200
3000

740

Figure 8a

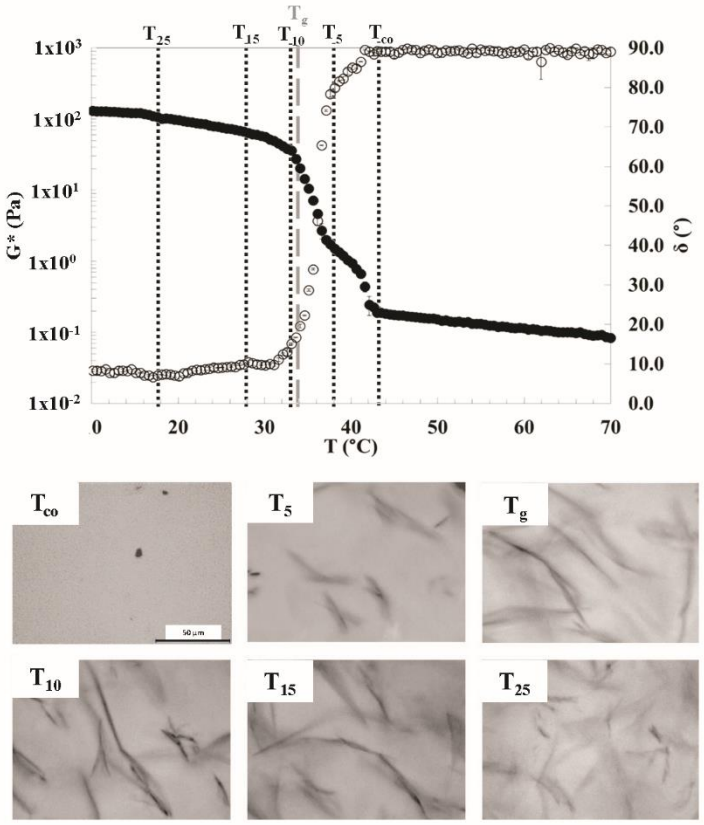

741

Figure 8b

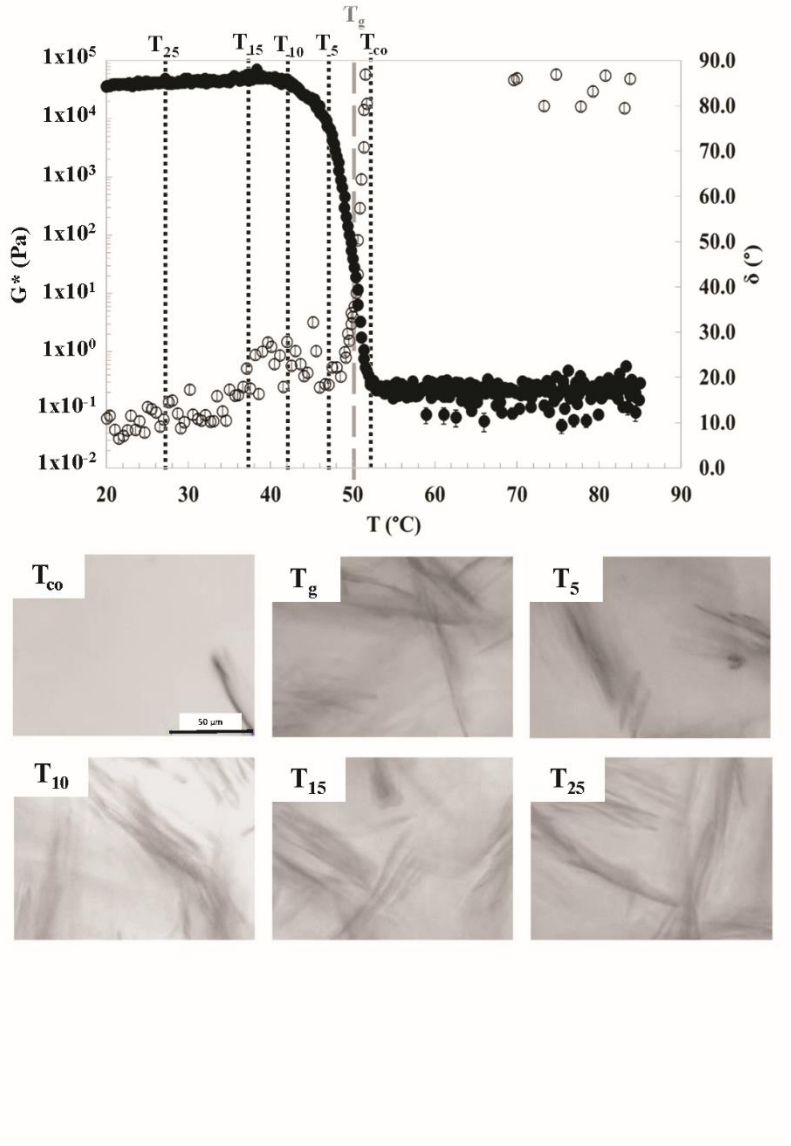

742

Graphical Abstract

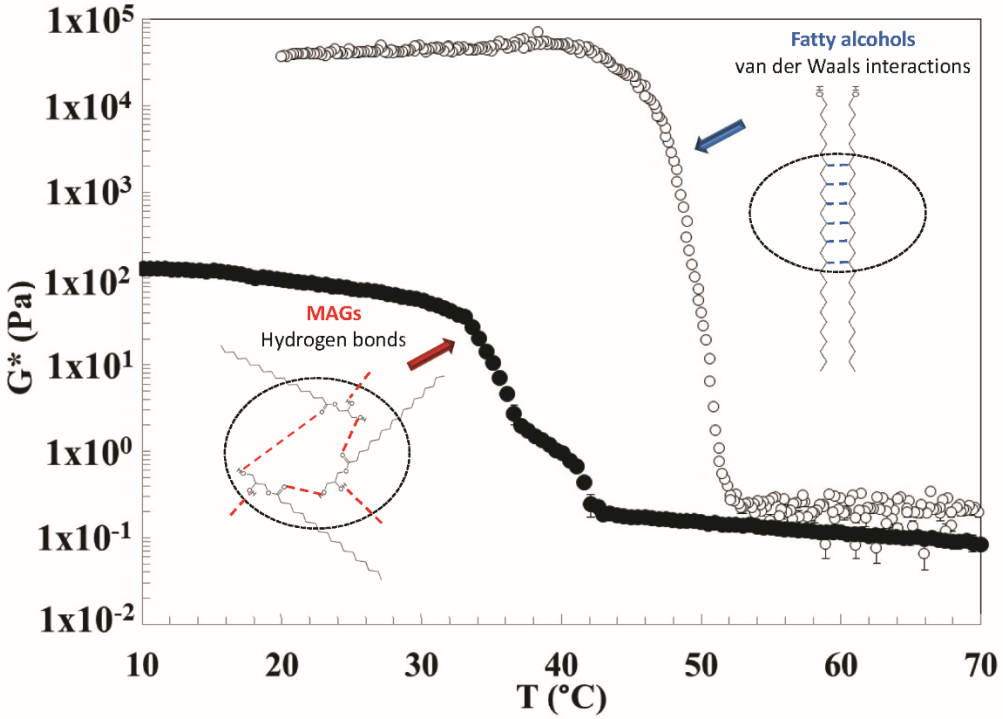

743

The effects of intermolecular interactions on the physical properties of organogels in edible oils

Francesca R. Lupi[1], *Valeria Greco*[1], *Noemi Baldino*[1], *Bruno de Cindio*[1], *Peter Fischer*[2], *Domenico Gabriele*[1]

[1] Department of Information, Modeling, Electronics and System Engineering, (D.I.M.E.S.) University of Calabria, Via P. Bucci, Cubo 39C, I-87036 Rende (CS), Italy

francesca.lupi@unical.it; valeria.greco@unical.it; noemi.baldino@unical.it, bruno.decindio@unical.it, domenico.gabriele@unical.it

[2] Institute of Food, Nutrition and Health, ETH Zurich, 8092 Zurich, Switzerland

peter.fischer@hest.ethz.ch

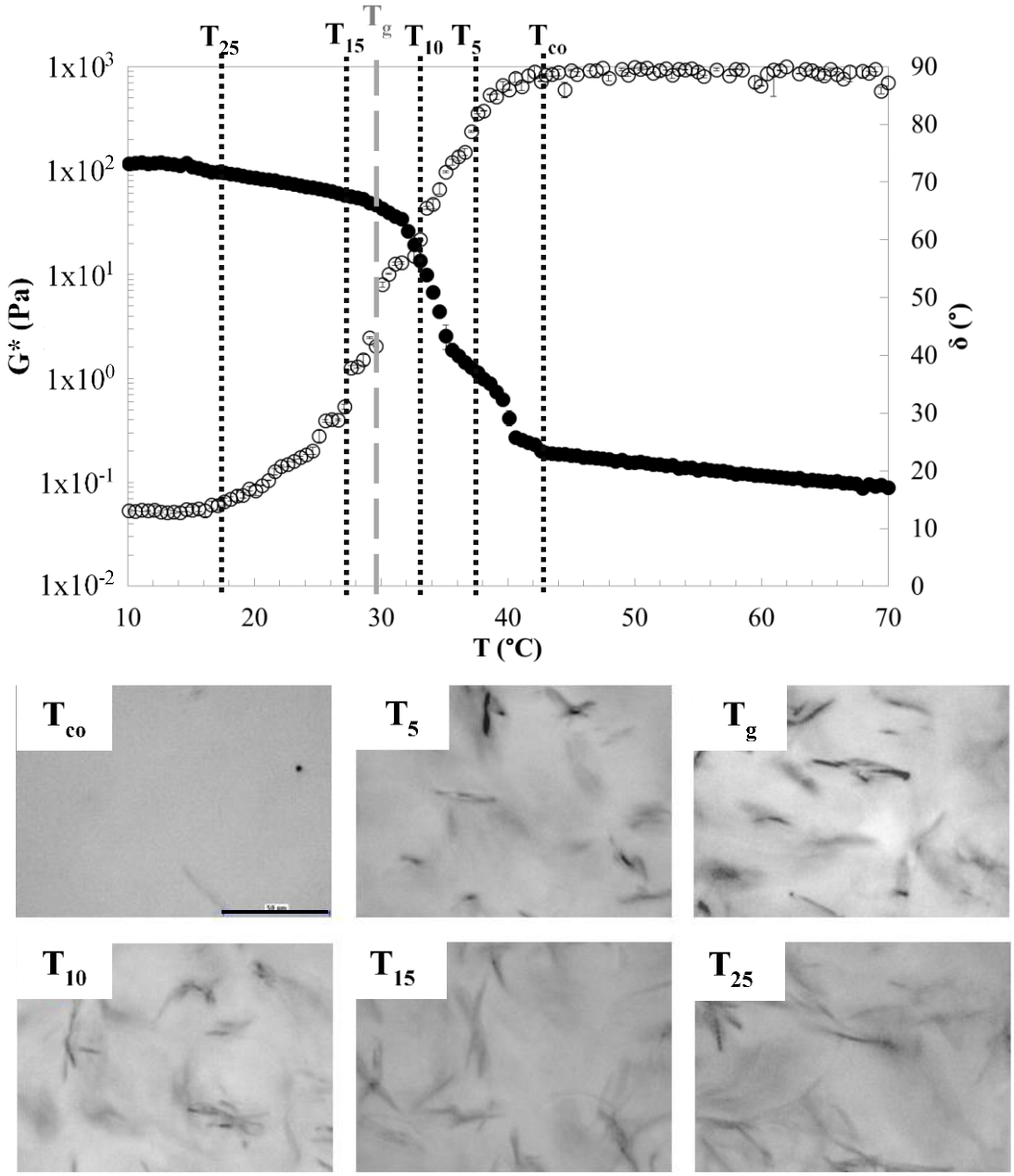

Figure S1 Time cure test for sample $VM_{0.030}$ in terms of G* (full symbols) and phase angle (white symbols). Dotted lines correspond to the different micro-photographs taken at T_{co}, T_5, T_{10}, T_{15} and T_{25}. Control bar in T_{co} micrograph is 50 μm.

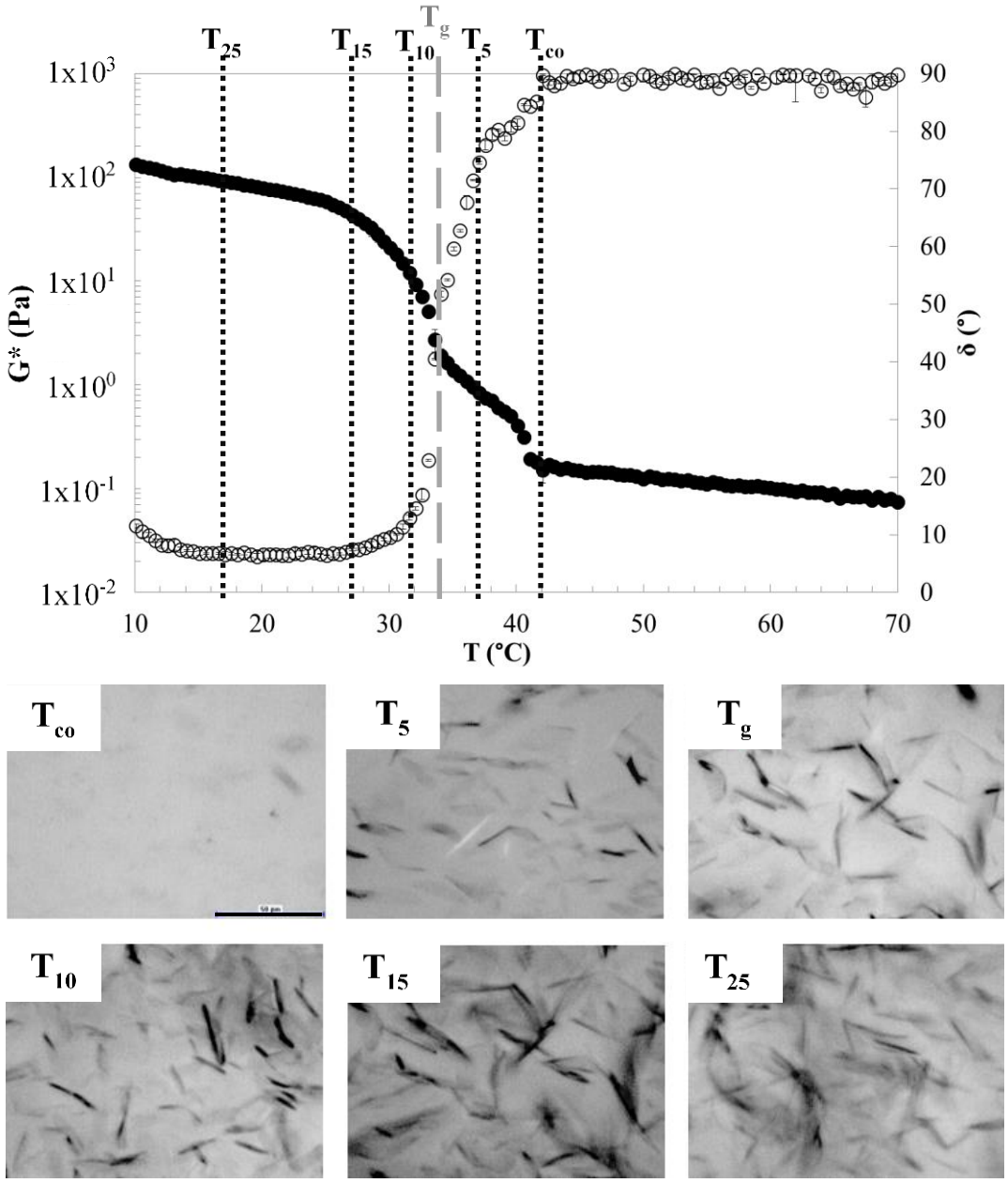

Figure S2 Time cure test for sample SM in terms of G* (full symbols) and phase angle (white symbols). Dotted lines correspond to the different micro-photographs taken at T_{co}, T_5, T_{10}, T_{15} and T_{25}. Control bar in T_{co} micrograph is 50 μm.

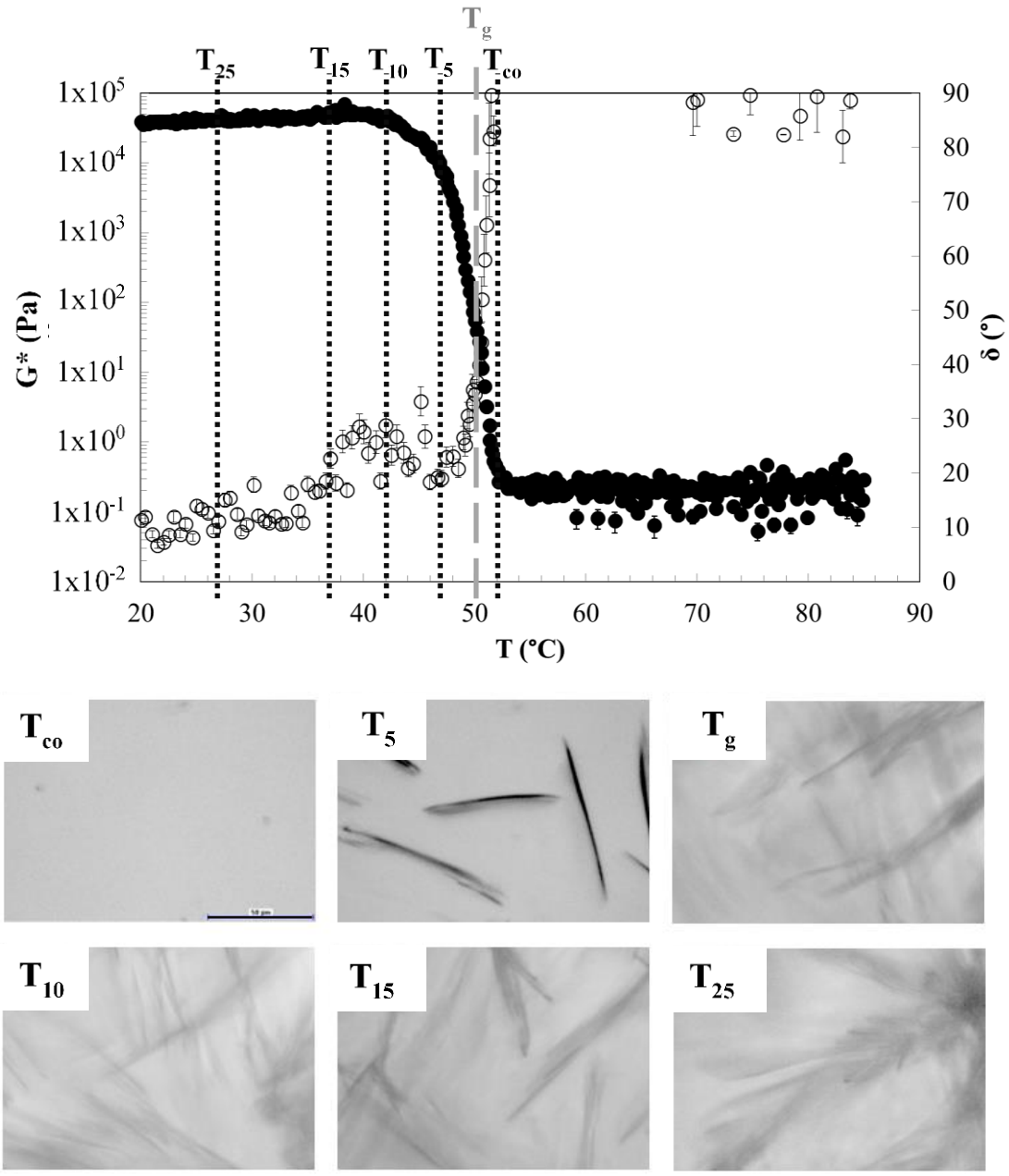

Figure S3 Time cure test for sample $VP_{0.030}$ in terms of G* (full symbols) and phase angle (white symbols). Dotted lines correspond to the different micro-photographs taken at T_{co}, T_5, T_{10}, T_{15} and T_{25}. Control bar in T_{co} micrograph is 50 µm.

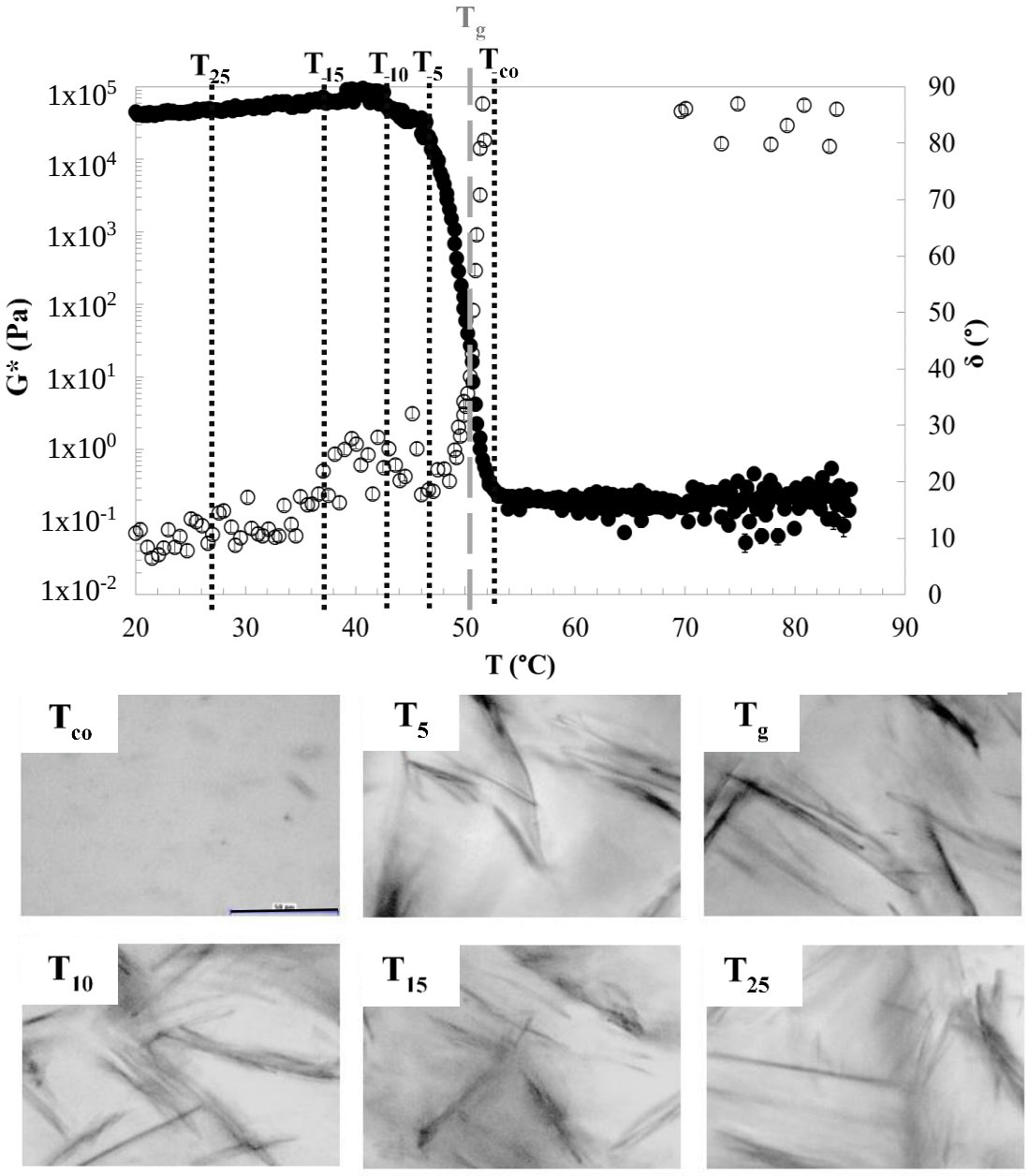

Figure S4 Time cure test for sample SP in terms of G* (full symbols) and phase angle (white symbols). Dotted lines correspond to the different micro-photographs taken at T_{co}, T_5, T_{10}, T_{15} and T_{25}. Control bar in T_{co} micrograph is 50 μm.